Influence of Magnetic Structure Size on Solar Irradiance Variations

Aman Priyadarshi Mukesh Kumar

Department of Astrophysical and Planetary Sciences
College of Arts and Sciences
University Of Colorado, Boulder

Defended on April 01, 2024

Committee Members:

Dr. Mark Rast (Advisor)
Department of Astrophysical and Planetary Sciences

Dr. Ann-Marie Madigan
Department of Astrophysical and Planetary Sciences

Dr. Abby Hickcox (Outside Reader)
Arts and Sciences Honors Program

Abstract

This thesis examines the interrelationship of the size of the magnetic structures on the Sun, particularly faculae, and the solar irradiance variations which are of significance for the understanding of the solar dynamics and the climate of the Earth. Using the high-resolution data coming from the Sunrise I Balloon-Borne Solar Observatory and the broader observations of the Precision Solar Photometric Telescope (PSPT), this study investigates the magnetic activity of the Sun and its nature, the implications, and the physics behind it. Through an analysis encompassing observational data and sophisticated MURaM simulations, the research delineates the nuanced interplay between magnetic field strength, structure size, and solar irradiance. Key findings highlight a significant correlation between the size of solar magnetic structures and their magnetic potency, offering new insights into the complex mechanisms driving solar luminosity variations. The study also deals with the methodological difficulties in comparing high-resolution observations with synthetic spectra and stresses the need to replicate the instrumental and atmospheric effects in simulations. The combination of observational and simulated data not only deepens our knowledge of solar magnetic fields but also highlights the possible effects of solar irradiance fluctuations on space weather and terrestrial climate systems. This thesis brings a considerable contribution to the field of solar physics by providing a holistic study of solar magnetic structures which in turn helps us to understand the Sun's role in the solar-terrestrial environment and the prospects for future research on solar dynamics and climate impact.

Dedication

To those who, in their quest for understanding, met only with silence yet never allowed their curiosity to be subdued—this work is dedicated to you.

From Nashik's warmth to Boulder's vast, open skies,
I ventured forth, where the universe's mysteries lie.
Homesickness shadowed, a constant, silent test,
Yet in celestial wonders, my heart found its quest.

Alone I landed, amidst the Rockies' grand embrace,
Friendships blossomed, lighting up my space.
Love found and lost, left my spirit bruised and sore,
Yet the stars whispered, "There's so much more."

In the depth of night, when despair seemed to win,
Family's love crossed oceans, felt deep within.
Boulder's bonds grew strong, a new family so kind,
In their support, a powerful solace I'd find.

Astrophysics, my beacon through the darkest nights,
Guided by its glow, I reached new heights.
This journey, woven with trials and love's spark,
Is a testament to resilience, a journey from the dark.

To my family in Nashik, who supported me from miles away, and to my friends in Boulder, who became my family, your unwavering belief in me lights every step of my path.

And to Shri. Baleshwar Prasad (1953-2021), my beloved grandfather, whose wisdom and love continue to guide me beyond the stars. I carry your legacy forward, with every success, every discovery.

Acknowledgements

Wow! It truly has been an amazing journey! It wouldn't be possible to walk this path alone and some of the individuals who were invaluable to me should be acknowledged as my guiding stars.

First off, a massive thank you to Dr. Mark Rast. You saw something in me even when I was scrambling to find my research footing. Your guidance wasn't just about the academic grind; you were there for the code struggles, the drafting dilemmas, and even those life's curveballs. You're not just my advisor; you've been a true mentor.

Big thanks to Dr. Ann-Marie Madigan for being a guiding light through the academic labyrinth. Your insights have been golden. And getting to hang in your group meetings was like getting a backstage pass to the cool kids' table in astrophysics—thank you for that privilege.

A huge shoutout to UROP for backing me with grants in the summers of 2022 and 2023. That financial boost was a game-changer and fueled my research when I needed it most.

Big thanks to the folks at LASP for not just the paycheck but for giving me a space that felt like my own little research haven. That cubicle and the work computer were more than just physical resources; they were where my best ideas came to life.

To Shivank Chadda, my partner in crime for those brain-fueling lunch breaks and endless science (and not-so-science) chats, you've been a constant through all the ups and downs.

And to Jacob Walter, Adel Al-Ghazwi, and Anish Kothari, my brothers from other mothers; becoming friends with you guys was like finding a home away from home. Our adventures and those life lessons we learned together? Priceless.

To those of you who have been part of this journey, regardless of whether I mentioned you here or not, thank you for all your support, encouragement, and faith in me—you made the difference.

Contents

1 Introduction and Background

1.1 Sun: The Closest Star

A star is a luminous celestial body primarily composed of hydrogen and helium. Through a process called nuclear fusion, stars convert hydrogen into helium, releasing vast amounts of energy in the form of light and heat. The Sun, our closest star, is a prime example of this process. At the sun's core, conditions become so intensely hot and pressurized, reaching temperatures of up to 29,000,000 degrees Fahrenheit and pressures about 100 billion times the atmospheric pressure on Earth, that hydrogen atoms come so close together they undergo nuclear fusion to release energy [1]. This energy radiates outward, powering the star and emitting the brilliance we observe. The sun has spent approximately 4.5 billion years converting half of its hydrogen core into helium [2]. Serving not only as the primary energy source for life on Earth, the Sun also stands as a cornerstone in solar and astrophysical research.

1.1.1 Characteristics and Importance

The Sun's sheer size and its dynamic processes play a crucial role in shaping solar phenomena. With a volume vast enough to encapsulate 1.3 million Earths, the Sun's large scale influences the intensity and frequency of solar events. Its surface, the photosphere, is an expanse of super-hot plasma, where the existence and combination of magnetic fields and convective movements give rise to various solar phenomena.

This plasma undergoes convection, a process where hot plasma rises to the surface, cools down, and then sinks back, creating a continuous cycle. This convective motion, combined with the Sun's rotation, is instrumental in the generation of its magnetic field. The magnetic field, in turn, is central to many of the Sun's most captivating features, such as sunspots and solar flares [3]. Sunspots, cooler regions on the Sun's surface, are areas of intense magnetic activity where the magnetic field inhibits convection, leading to reduced surface

temperatures. Solar flares, on the other hand, are explosive events caused by the release of magnetic energy stored in the Sun's atmosphere.

The size and complexity of the Sun's convective processes also contribute to its uniqueness as an astrophysical object. Solar convection not only controls the magnetic field but also drives the Sun's explosive events, influences the interplanetary medium, and impacts Earth's weather and space weather. Near the solar surface, granulation patterns, driven by convection, play a pivotal role in solar dynamics. The study of these granulation patterns and larger-scale convective motions offers invaluable insights into the solar dynamo, a key component in understanding the Sun's magnetic behavior and various astrophysical processes [5].

Understanding the Sun's characteristics and their impacts on solar phenomena not only advances our knowledge of solar physics but also enhances our understanding of stellar dynamics in general, making the Sun a unique and vital object of study in astrophysics.

1.1.2 Solar and Magnetic Activity

The Sun's magnetic field, both complex and dynamic, emerges from its internal dynamo processes, which are directly linked to the convective motion of plasma and the Sun's differential rotation. Differential rotation, as explained in Figure 1, refers to the phenomenon where different parts of the Sun rotate at varying speeds; the equator rotates faster than the poles. This variation in rotation speeds causes the plasma within the Sun to twist and shear, contributing significantly to the generation and evolution of its magnetic field [3].

Central to the Sun's magnetic complexity is the dynamo mechanism. This process involves the conversion of the Sun's kinetic energy, arising from its rotation and convection, into magnetic energy. The movement of the Sun's electrically conductive plasma generates electric currents, which in turn produce and continuously reshape the magnetic fields. This dynamic process is responsible for the ever-changing nature of the Sun's magnetic field, resulting in its continual evolution and reconfiguration [6].

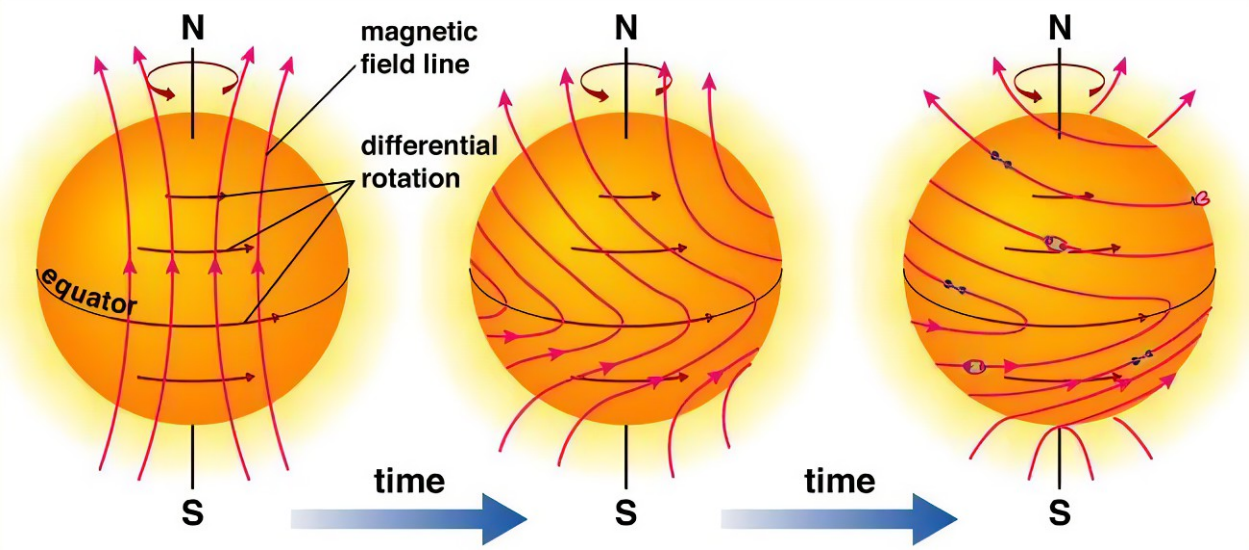

Figure 1: Differential rotation winds up the Solar magnetic field. Image borrowed from The Essential Cosmic Perspective, by Bennett et al.

The impact of these magnetic fields is evident in various solar surface and atmospheric phenomena. In active regions, the magnetic fields intensify the brightness of active areas, especially near the solar limb. This intensification is a direct consequence of the magnetic fields modulating the heat transfer process of convection, which in turn can increase the heating of the chromosphere and corona [7]. Solar oscillations, too, are influenced by these magnetic interactions, as the magnetic fields alter the size of the resonant cavity, thereby modifying the oscillations' frequency.

Sunspots: As key indicators of the Sun's magnetic activity, sunspots, as shown in Figure 2, are cooler, darker regions on the solar surface. They form in areas where intense magnetic fields disrupt the normal convective flow of energy from the Sun's interior, leading to a decrease in surface temperatures. Sunspots typically have temperatures ranging from 3,000 to 4,500°C and vary in size from small spots to large complexes. They are often the sites of other dynamic solar events, including solar flares and coronal mass ejections, and are integral to understanding the solar magnetic cycle [8].

Faculae: Contrasting with sunspots, faculae are brighter areas on the Sun's surface, forming in regions with high magnetic field concentrations. These areas heat up due to the

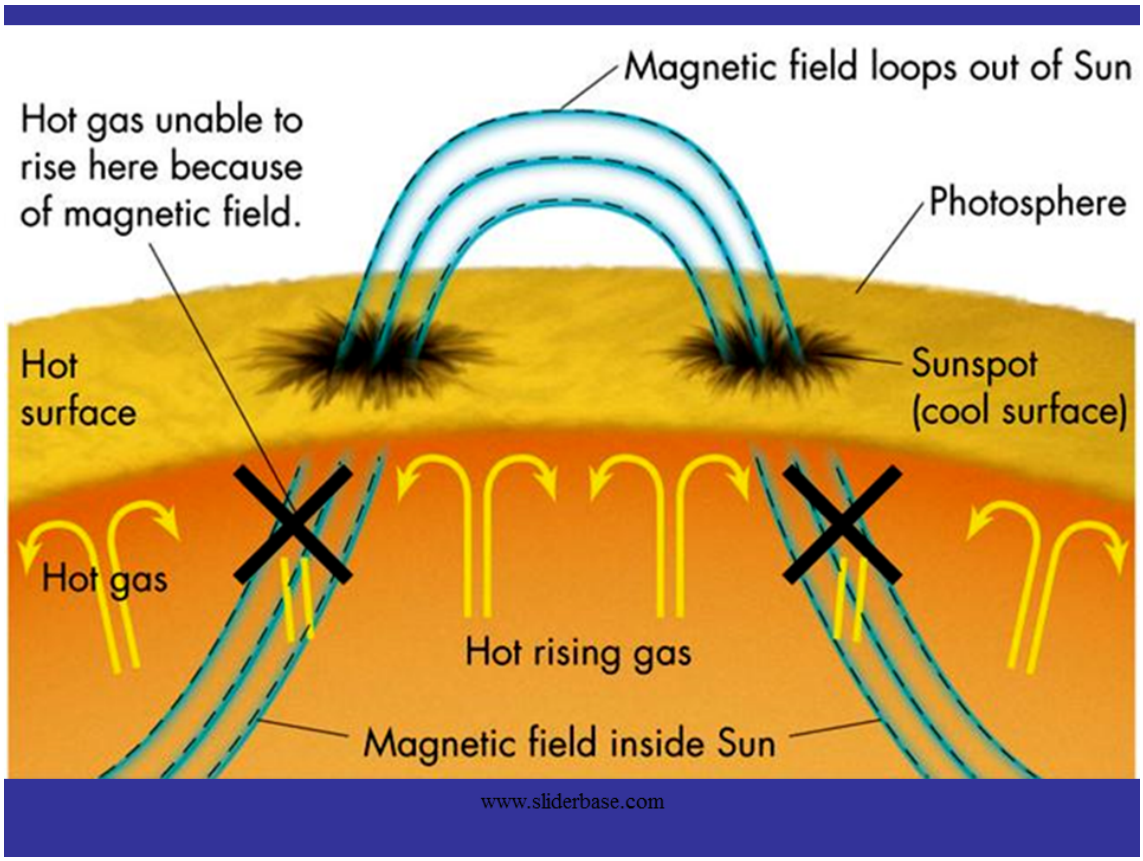

Figure 2: Sunspots appear darker due to inhibited convection caused by intense magnetic fields. The reduction in plasma flow leads to lower temperatures in these regions.

magnetic suppression of cooler plasma transport, leading to increased brightness. Faculae are particularly prominent during periods of high solar activity and play a crucial role in influencing the Sun's overall brightness and, consequently, solar irradiance variations that can affect Earth's climate [9].

1.1.3 Implications of Solar Activity

The Sun's radiative output, a critical factor for Earth's climate, is significantly influenced by the dynamic interplay between sunspots and faculae. Sunspots, with their cooler temperatures, can reduce solar output, while faculae, being brighter, tend to increase it. Despite sunspots tending to make the Sun appear darker, faculae cause it to look brighter. In fact, during a sunspot cycle, the faculae outweigh the effects of sunspots, making the Sun appear

slightly (about 0.1 percent) brighter at sunspot maximum than at sunspot minimum. These are also magnetic areas, but the magnetic field is concentrated in much smaller bundles than in sunspots (see Figure 3). This balance between dark and bright regions on the Sun's surface leads to variations in solar brightness, or solar irradiance, which directly impacts Earth's climate systems. Such variations can lead to notable climate phenomena, affecting both short-term weather patterns and long-term climatic trends [10].

In addition to these irradiance variations, the Sun's magnetic disturbances, such as solar flares and coronal mass ejections (CMEs), present significant challenges for space exploration and technology. Solar flares, which are intense bursts of radiation, can disrupt radio communications and navigation systems. They are also known to produce high-energy particles that can be hazardous to astronauts and satellite electronics [11].

Coronal mass ejections, on the other hand, involve massive bursts of solar plasma and magnetic field into space, which can interact with Earth's magnetosphere, leading to geomagnetic storms. In 1989, most of Quebec was darkened for more than 12 hours by blackouts caused when a massive solar storm shut down the province's power grid. Radio transmissions were also scrambled, These storms can induce electrical currents in long conductors on Earth's surface, such as power lines, potentially leading to widespread power outages. Moreover, they pose a risk to spacecraft, including damaging sensitive electronics and disrupting satellite operations [12].

A comprehensive understanding of solar magnetic activity is thus crucial not only for advancing astrophysical research but also for preparing and protecting our technological infrastructure against solar-induced disturbances. Studies in solar physics provide critical insights into space weather forecasting, which is essential for mitigating the impacts of solar activity on Earth's technological systems and for ensuring the safety of astronauts in space [13].

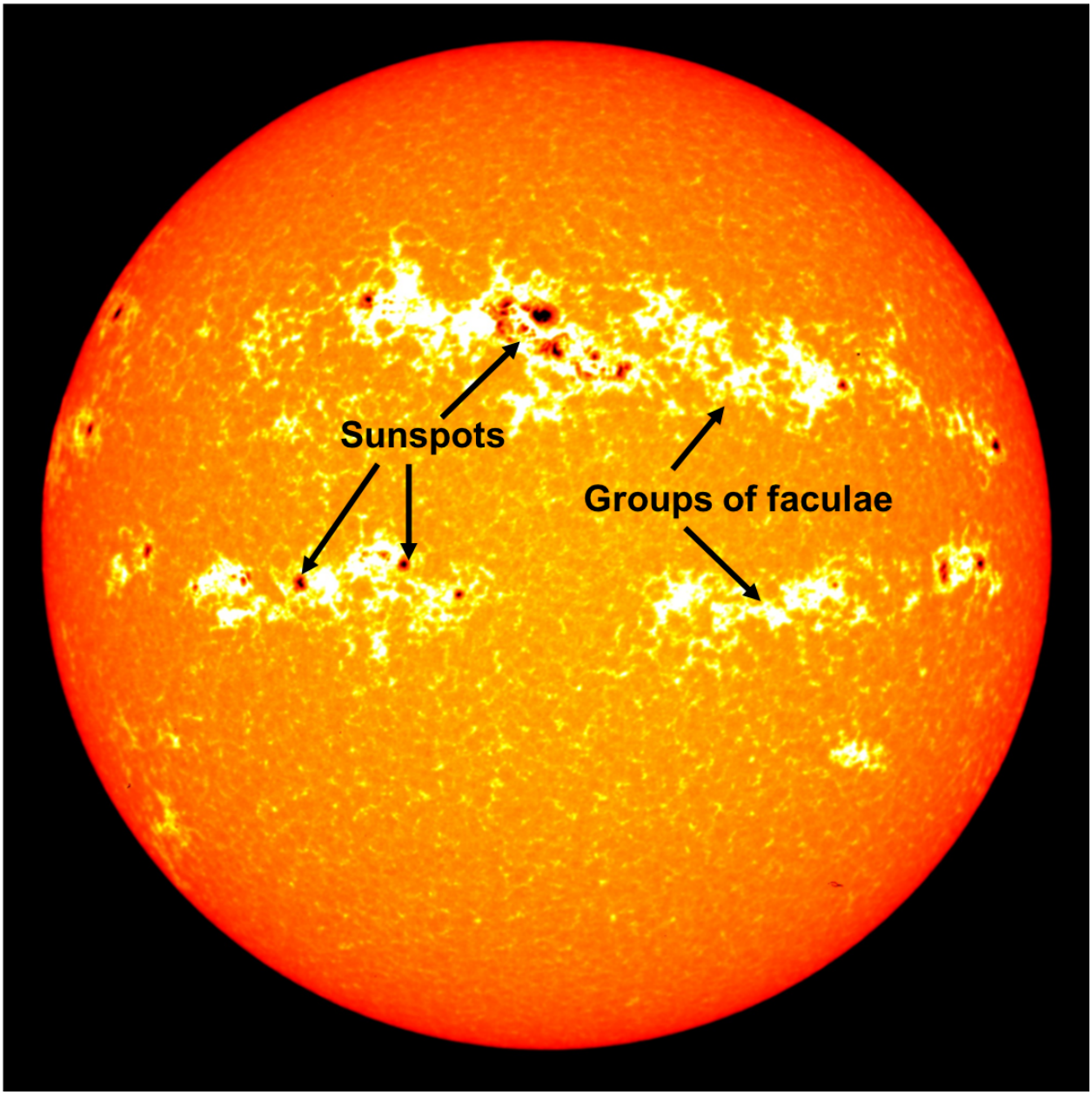

Figure 3: The Sun showcasing both sunspots and faculae. The cooler, darker sunspots contrast with the brighter faculae, which ultimately dominate the solar luminosity cycle, leading to a net increase in brightness during sunspot maxima. Image credit: NASA/Goddard Space Flight Center Scientific Visualization Studio.

1.2 Motivation

While the Sun's broader characteristics are well-documented, it is the finer, smaller-scale magnetic structures, such as faculae and plage, that hold key insights into understanding

solar physics. This research delves into these smaller structures, aiming to unravel their intricate roles in solar phenomena.

A primary focus of this study is to explore the relationship between the size of these solar structures, their magnetic field strength, and the resulting impact on solar brightness. Faculae, the bright spots discernible on the solar surface, are known to significantly influence the Sun's radiative output. By analyzing high-resolution data from the Sunrise I mission of 2009 and Precision Solar Photometric Telescope (PSPT) data from 2005 and then comparing it with profiles generated from Max Planck/University of Chicago Radiative MHD (MURaM) simulations, this research seeks to illuminate the intricate ways these structures contribute to the Sun's overall brightness and their involvement in solar magnetic activities [14, 15].

The implications of this research extend beyond academic curiosity. The Sun's radiative output is critical in Earth's climatic systems. Figure 4 clearly shows that even minor variations in solar irradiance can lead to noticeable climatic changes on Earth. Understanding the dynamics of solar structures and their magnetic fields is crucial for predicting solar activities and their potential effects on Earth's environment [10].

As shown in Figure 4, the variations in the Total Solar Irradiance (TSI), although small (about 1361-1362 watts per square meter), can have significant climatic implications on Earth. For instance, periods of low solar activity have been historically linked to cooler climatic conditions on Earth. The discrepancies between the different data sets (ACRIM, PMOD, RMIB, TIM) highlight the challenges in measuring solar irradiance with absolute precision due to differences in instrument calibration and methodologies. Nonetheless, these measurements are crucial inputs for climatological models aimed at predicting how slight changes in solar energy affect Earth's climate, alongside other factors such as greenhouse gases and volcanic activity.

Furthermore, this research underscores the advancement of observational and simulation methodologies in astrophysics. The combination of observational data and MURaM simulations presents an exceptional opportunity to cross-validate theoretical models with empirical

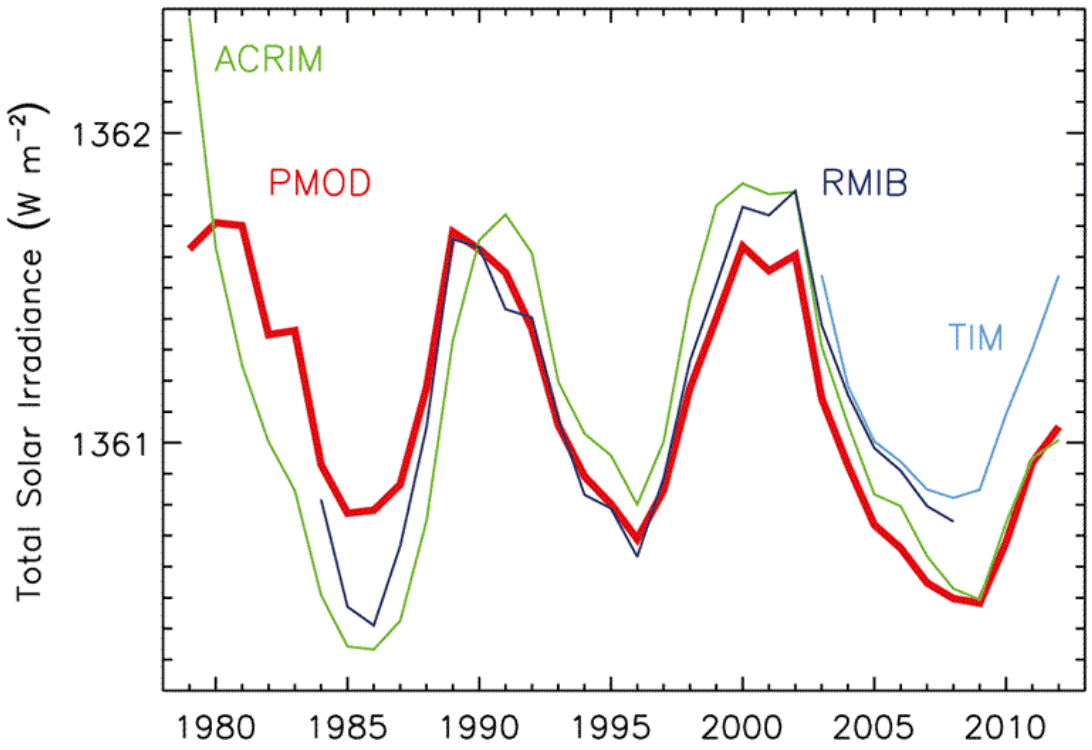

Figure 4: These annual, average TSI measurements were compiled by the Active Cavity Radiometer Irradiance Monitor (ACRIM), the Physikalisch Meteorologisches Observatorium/World Radiation Center (PMOD), the Royal Meteorological Institute of Belgium (RMIB), and Total Irradiance Monitor (TIM). TSI represents the amount of solar energy received by Earth per square meter at the top of the atmosphere. These data shows that the Sun's output isn't constant but varies slightly over time, in sync with the 11-year solar cycle marked by peaks (solar maxima) and troughs (solar minima) corresponding to changes in solar magnetic activity. IPCC AR 5 Source: www.ucsusa.org

data. This comparison between observation and simulation is vital for ensuring that our theoretical understanding of solar phenomena remains anchored in reality, while continuously enhancing our comprehensive knowledge of the Sun [16].

1.3 Observations vs Simulations

Understanding the Sun requires a multifaceted approach, encompassing both observational and simulation methodologies. Observational studies involve direct examination of the Sun using various instruments such as ground-based telescopes, space-based satellites

like the Solar Dynamics Observatory (SDO), and specialized missions like the Parker Solar Probe. These methods offer real-time data, capturing the Sun's activities in their immediate form. Over the years, observational data have led to pivotal discoveries, from the detailed structure of sunspots to the dynamic processes underlying solar flares and coronal mass ejections [17].

In this context, we specifically chose to use data from the Sunrise mission of 2009 due to its unique high-resolution observations of the solar atmosphere. Additionally, to complement the high-resolution data from Sunrise, we incorporated observations from the Precision Solar Photometric Telescope (PSPT) from 2005. The PSPT data provide a broader perspective by offering consistent solar imaging and capturing the Sun's irradiance variations over an extended period, thereby enhancing the robustness of our findings through a comparative analysis [18]. This combined dataset provides unparalleled insights into the fine-scale structures and dynamics of the Sun, crucial for our study and not available in such detail from other solar observations.

Complementing observational studies are simulations, which employ advanced computational models to replicate solar processes. These simulations, like those conducted using the MURaM code, enable scientists to explore and understand complex solar phenomena that may not be easily observed, such as the very complex interactions within sunspots or the detailed dynamics of magnetic reconnection during solar flares [15]. Simulations provide an environment where variables can be controlled and manipulated, offering insights into the fundamental physics driving solar activities.

While observations offer direct and tangible evidence of solar phenomena, they are sometimes constrained by the limitations of current technology and can be influenced by intervening variables, such as Earth's atmosphere or the positioning of observational equipment. On the other hand, simulations are grounded in our current theoretical understanding, and their accuracy depends on the assumptions and models used. As a result, they may not always capture the full spectrum of solar complexity.

A synergistic approach that combines observations and simulations is therefore crucial in solar physics. Observations serve to guide and validate the simulations, ensuring that the models reflect reality. Conversely, simulations provide theoretical insights and predictions that can be verified through observational data. This integrated methodology allows for a more comprehensive and nuanced understanding of the Sun. It ensures that the strengths of each approach are maximized while compensating for their limitations, thereby painting a more complete picture of solar dynamics and informing future research directions.

2 Observations

2.1 Sunrise I Balloon-Borne Solar Observatory

Sunrise I, a pioneering solar observatory (Figure 5), was specifically designed for high-resolution, spectro-polarimetric observations of the Sun's atmosphere. The observatory's central feature was its 1-meter aperture main telescope, which fed data into three sophisticated focal-plane instruments: the spectrograph-polarimeter (SP), the filter graph (FG), and the magnetograph. The primary scientific objective of Sunrise I was to delve into the intricate structure and dynamics of the solar atmosphere's magnetic field, particularly within the chromosphere, and to unravel the underlying physics of solar irradiance changes [14].

Figure 5: Sunrise 1 immediately before launch. Figure from [14].

The observatory's design aimed to achieve high spatial resolution, down to 0.055 arcseconds, which necessitated a complex pointing and guiding system. Additionally, Sunrise I

was equipped with a state-of-the-art wavefront control system, allowing for precise in-flight alignment capabilities, essential for capturing high-quality data.

Launched on June 8, 2009, from the European Space Range in Kiruna, Sweden, the Sunrise I mission spanned 5 days, 17 hours, and 18 minutes. It concluded with a landing on Somerset Island in Nunavut, Canada. The mission's success was marked by the wealth of data collected, which continues to provide critical insights into the Sun's ultraviolet radiation and its impact on the polar stratosphere's chemistry [19].

2.1.1 Mission Objectives

The central aim of the Sunrise project was to comprehend the structure and dynamics of the solar atmosphere's magnetic field, a fundamental driver of solar activity. This magnetic field is not only instrumental in shaping the solar atmosphere but also plays a crucial role in governing Earth's space environment. Moreover, variations in this magnetic field can influence the variability of solar irradiance, potentially leading to significant impacts on Earth's long-term climate [16, 20].

One of the key challenges in solar physics has been understanding the intense magnetic field concentrations in the solar photosphere, especially on spatial scales below 100 km. These small-scale magnetic structures are critical for the dynamics and energetics of the entire solar atmosphere, influencing everything from solar flares to coronal mass ejections. However, studying these structures from ground-based observatories has been hindered by atmospheric turbulence, which distorts the images.

Sunrise was uniquely positioned to overcome this limitation. Carried by a huge helium balloon, Sunrise operated at 35-40 km above the Earth's atmosphere leaving most of the Earth's atmosphere underneath. It provided an unprecedented opportunity to observe these small-scale magnetic structures on their intrinsic spatial and temporal scales. The mission's primary objective was to capture high-resolution measurements of the magnetic structure in the solar atmosphere, offering new insights into the mechanisms of solar magnetism and its

broader implications for solar-terrestrial relations [14].

2.1.2 Mission Achievements

Since its inaugural flight in 2009, the Sunrise telescope has marked a series of significant achievements in solar observation. Operated during stratospheric balloon flights, Sunrise successfully obtained diffraction-limited image quality, which was crucial for detailed solar studies. One of the key accomplishments of the mission was its ability to study the UV spectral region down to 220 nm. This spectral range is particularly important for understanding the Sun's atmosphere but is inaccessible from ground-based observatories due to atmospheric absorption.

The data collected by Sunrise during these flights has been instrumental in advancing our knowledge of solar magnetic fields and their influence on solar irradiance and atmospheric dynamics. The high-altitude vantage point of the balloon flights allowed for unmatched observations of small-scale magnetic structures and their interactions in the solar atmosphere, providing new insights into solar magnetic activity and its effects on space weather.

Furthermore, the success of Sunrise has established a strong foundation for future solar observatories. Its achievements in capturing high-resolution images and studying previously inaccessible spectral regions demonstrate the potential of balloon-borne and space-based observatories in pushing the frontiers of solar physics. This experience positions Sunrise as a pivotal element in the conception and design of future space-borne solar observatories, which could provide even more detailed and comprehensive data on solar activities [14].

2.1.3 Instruments

The Sunrise observatory's instrumentation was meticulously designed to optimize solar observation capabilities. The array of instruments included:

- A lightweight solar telescope featuring a 1 m aperture, enabling high-resolution imaging and capturing fine details of the solar atmosphere.

- The Spectrograph-Polarimeter (SUPOS), which facilitated precise measurements of spectral lines in both linear and circularly polarized light. This instrument was crucial for understanding the magnetic field structure and dynamics by analyzing the polarization of sunlight [21].

- The Filtergraph (SUFI), offers high-resolution imaging capabilities in both visible and UV spectral ranges. This instrument played a vital role in studying various layers of the solar atmosphere and their interactions.

- The Imaging Magnetograph eXperiment (IMaX), which provided two-dimensional maps of the complete magnetic field vector and the line-of-sight velocity. IMaX's data has been instrumental in advancing our understanding of solar magnetic phenomena, particularly in the photosphere [16].

Additionally, the telescope was equipped with a state-of-the-art control system, including a wavefront sensor for precise alignment and focus adjustments. Image stabilization was achieved through a correlation tracker that controlled a high-speed steering mirror, ensuring sharp and clear observations even during the balloon's movement. These technological advancements have contributed significantly to the success of the Sunrise mission, enabling detailed and high-quality solar observations.

2.1.4 Stokes Parameters: Decoding Solar Polarization

A comprehensive analysis of solar magnetic fields in this research is grounded in the combined use of Stokes Parameters and the Zeeman Effect. These methodologies are indispensable in deciphering the complexities of the Sun's magnetic properties through the study of polarized light.

Stokes Parameters, comprising I, Q, U, and V, are key to interpreting the polarization state of solar light:

$$\begin{pmatrix} I \\ Q \\ U \\ V \end{pmatrix}$$

Each component offers unique insights:

- I measures the total light intensity, serving as a fundamental reference.
- Q and U represent linear polarization components, critical for understanding the magnetic field's plane-of-sky orientation.
- V corresponds to circular polarization, revealing the line-of-sight component of the magnetic field.

Instruments like the Imaging Magnetograph eXperiment (IMaX) on Sunrise exploit these parameters to analyze light polarization induced by solar magnetic fields. The extracted data is pivotal for mapping magnetic field vectors across sunspots, faculae, and other solar features [16].

2.1.5 The Zeeman Effect: Probing Solar Magnetic Fields

The Zeeman Effect, a key phenomenon in solar astrophysics, occurs when magnetic fields cause the splitting of spectral lines. This effect is observable through two distinct patterns:

1. **Normal Zeeman Effect**: Observed in weak magnetic fields, it results in the splitting of a spectral line into $2l + 1$ evenly spaced components, where l is the orbital quantum number of the electron.
2. **Anomalous Zeeman Effect**: Occurring in stronger magnetic fields, this effect produces more complex splitting patterns due to the interaction of the electron's spin with its orbital motion.

By applying spectro-polarimetric methods, like those used in IMaX, to observe the Zeeman-induced line splitting, the magnetic field's strength and orientation in the solar atmosphere can be accurately determined. This technique complements the information obtained from Stokes Parameters, providing a holistic view of solar magnetic activities [22].

2.1.6 Integrating Stokes Parameters and the Zeeman Effect in Research

This research leverages these tools to systematically examine the magnetic structures within the solar atmosphere and their impact on solar irradiance. The process involves:

1. Capturing polarization data using IMaX.
2. Analyzing Stokes Parameters to map the magnetic fields.
3. Utilizing the Zeeman Effect for detailed measurements of magnetic field strength and direction.
4. Correlating these findings with changes in solar brightness, thereby enhancing our understanding of solar-terrestrial interactions and space weather dynamics.

This integrated approach not only enriches the study of solar magnetic fields but also contributes significantly to the broader understanding of solar influence on Earth's climate systems.

2.2 Precision Solar Photometric Telescope (PSPT)

The Precision Solar Photometric Telescope (PSPT) represents a pivotal tool in solar observation, primarily focusing on high-precision photometric and polarimetric measurements of the solar atmosphere. Unlike the high-resolution, targeted observations of Sunrise I, PSPT provides comprehensive, full-disk images of the Sun, capturing global solar phenomena and long-term variations in solar irradiance and magnetic fields [18].

2.2.1 Overview and Objectives

The Precision Solar Photometric Telescope (PSPT) employs a dual-channel design to capture high-resolution images in the blue continuum (409.412 nm), red continuum (607.095 nm), and the Ca II K (393.415 nm) line. This setup facilitates a comprehensive analysis of the solar photosphere and chromosphere. PSPT's primary objective centers on the long-term, high-precision monitoring of solar surface brightness variations across these spectral lines. Such observations are pivotal in dissecting the dynamics of the solar cycle, elucidating the mechanisms behind solar irradiance changes, and assessing their subsequent impacts on Earth's climate. While PSPT contributes valuable data regarding the solar atmosphere, its design is more attuned to photometric accuracy and solar irradiance studies rather than detailed magnetic field mapping, which often requires specialized magnetographic instruments [23].

2.2.2 Data Collection and Processing

PSPT is equipped with a 15 cm refracting telescope that, in conjunction with a narrow-band filter system, enables the collection of high-resolution, full-disk solar images. This telescope setup achieves a spatial resolution capable of finely resolving distinct solar features such as sunspots, faculae, and granulation patterns, which are critical for understanding solar dynamics and variability.

The data collection process with PSPT involves a series of steps to ensure photometric accuracy, which is paramount for detecting subtle variations in solar brightness. Initially, the telescope acquires images in the blue continuum, red continuum, and the Ca II K line, each offering unique insights into different layers of the solar atmosphere. The blue and red continuum images are particularly useful for studying the photosphere, while the Ca II K images probe the chromosphere's dynamics.

To maintain high photometric precision, PSPT undergoes regular calibration sessions using pre-defined photometric standards. This calibration process is essential for correcting

any systemic biases in the measurements, ensuring that the observed brightness variations are truly solar in origin and not artifacts of the instrumentation or observational conditions.

Furthermore, PSPT employs advanced atmospheric correction techniques to mitigate the effects of Earth's atmosphere on the observed solar images. Atmospheric turbulence and differential absorption can distort the solar features and affect the photometric accuracy. By applying sophisticated image processing algorithms, PSPT corrects for these atmospheric disturbances, enhancing the clarity and reliability of the solar observations.

The processed data from PSPT, characterized by its high photometric accuracy and stability, serves as a valuable resource for studying long-term solar irradiance variations. The comprehensive full-disk images captured by PSPT provide a global view of the Sun's behavior over time, complementing the detailed but localized observations from other solar telescopes like Sunrise I [24, 18].

This approach to data collection and processing enables PSPT to contribute significantly to our understanding of solar phenomena, particularly in the context of solar irradiance variations and their potential impact on Earth's climate system.

3 Simulations

3.1 Features and capabilities

MURaM (Max Planck Institute for Solar System Research/University of Chicago Radiation Magneto-hydrodynamics code) stands out as a sophisticated 3D magnetohydrodynamics simulation tool, specifically engineered for probing the dynamics of the solar convection zone and photosphere. It's an integral asset for simulating the complex interplay between magnetic fields and solar atmospheric processes [15].

3.1.1 Technical Framework and Innovations

Key technical features of MURaM include:

- **Radiative Transfer Module**: This non-local and non-grey module is crucial for accurately modeling the interactions between radiation and magnetic fields, a pivotal aspect of solar atmosphere dynamics.
- **Partial Ionization Effects**: MURaM's simulations account for partial ionization, significantly affecting magnetic field behavior in the solar photosphere and chromosphere.
- **Parallelization for Advanced Computing**: Its domain decomposition parallelization enables efficient operation on large-scale, massively parallel supercomputers, facilitating high-resolution solar simulations.

3.1.2 Modeling Capabilities

MURaM's ability to simulate detailed solar phenomena is crucial for advancing our understanding of solar magnetism. From the emergence of sunspots to the intricate dynamics within solar plages, MURaM's high-resolution simulations provide essential insights into the solar magnetic field's behavior and its influence on solar phenomena [15].

The capabilities of MURaM make it a vital tool in the field of solar physics, allowing for a deep exploration of the mechanisms driving magnetic activity in the Sun's atmosphere.

3.2 Applications

The MURaM code represents a significant advancement in the field of solar physics. This state-of-the-art simulation tool is specifically designed for in-depth study of the Sun's outer layers, focusing on the magnetohydrodynamics (MHD) of the solar photosphere and the upper layers of the convection zone.

3.2.1 Simulating Solar Photosphere and Convection Zone

MURaM's simulations extend our understanding of solar phenomena in several key areas:

1. **Sunspot Formation and Evolution**: By simulating the complex dynamics of magnetic fields in the solar photosphere, MURaM provides insights into the formation, development, and decay of sunspots. These simulations help explain how sunspots, the visible manifestations of concentrated magnetic fields, evolve and influence solar irradiance.

2. **Solar Granulation**: MURaM effectively models the granulation patterns observed on the solar surface. These granules, caused by convective currents, play a crucial role in the transport of energy from the Sun's interior to its surface. Understanding granulation is essential for comprehending the Sun's energy output and its variation [25].

3. **Magnetic Flux Emergence**: The code simulates the emergence of magnetic flux from the deeper layers of the convection zone to the photosphere. This process is vital for understanding the solar magnetic cycle and its implications for solar activity, including solar flares and coronal mass ejections.

3.2.2 Advancing Solar Irradiance Research

In the context of this research, MURaM's simulations are invaluable for exploring the relationship between solar magnetic activity and solar irradiance. By simulating the small-scale magnetic structures and their interaction with the solar atmosphere, MURaM contributes to a deeper understanding of how these structures influence the Sun's radiative output. This aspect is particularly significant for predicting solar activity's impact on space weather and terrestrial climate systems.

The versatility and precision of MURaM's simulations make it an indispensable tool in solar physics, enabling researchers to model complex solar phenomena with unprecedented accuracy. Its contributions extend beyond theoretical research, offering practical insights for future solar observations and space missions.

3.3 Future prospects

The ongoing advancements in computational technology promise a bright future for MURaM simulations in solar physics. As computational power continues to increase, we can expect MURaM to achieve even higher resolutions and incorporate more complex physical processes in its simulations.

3.3.1 Enhanced Resolution and Complexity

Future developments in MURaM may include:

- **Higher Resolution Simulations**: With the advent of more powerful computing resources, MURaM can produce simulations at even finer scales. This will allow for a more detailed analysis of small-scale magnetic structures and their interactions within the Sun's atmosphere, providing clearer insights into phenomena like magnetic reconnection and flux emergence.

- **Incorporation of Additional Physical Processes**: Future versions of MURaM

could integrate more comprehensive physics, such as advanced treatments of plasma dynamics and radiative transfer. This would enable more accurate modeling of solar phenomena, particularly in simulating the Sun's outer layers [26].

3.3.2 Implications for Solar Research and Space Weather Prediction

The enhancement of MURaM's capabilities will have significant implications for solar research:

1. **Understanding Solar Magnetic Activity**: Higher resolution simulations will provide deeper insights into the origins and evolution of solar magnetic activity, contributing to our understanding of the solar cycle and its variability.

2. **Space Weather Prediction**: Improved simulations will enhance our ability to predict space weather events, such as solar flares and coronal mass ejections, which are critical for safeguarding satellite operations and communication systems on Earth.

3. **Solar-Terrestrial Environment**: As MURaM simulations become more sophisticated, they will offer more accurate predictions of the Sun's influence on the broader solar-terrestrial environment, including impacts on Earth's climate and the heliosphere.

The evolution of MURaM simulations stands to significantly advance our comprehension of solar phenomena and their implications, reinforcing the importance of computational simulations in astrophysics research.

3.4 Synthetic spectra from MURaM

Synthesizing spectral lines from MURaM simulation outputs is a critical step in validating the simulations against actual observational data. This synthesis process involves generating artificial spectral profiles based on the physical conditions predicted by the simulations.

3.4.1 Significance of Spectral Line Synthesis

The synthesis of spectral lines is crucial for a few key reasons:

- **Comparative Analysis**: It enables direct comparison between simulated and observed solar spectra, offering a way to validate and refine the simulations.
- **Understanding Solar Atmosphere**: Spectral lines, particularly those forming in the cooler gas regions of the Sun's photosphere, provide insights into the solar atmosphere's structure and dynamics.

Given that the MURaM code calculates various properties like vertical velocity across the simulation domain, an additional layer of processing is necessary to transform these physical parameters into observable spectral lines.

3.4.2 Employing the Rybicki-Hummer (RH) Spectral Synthesis Code

For this research, the Rybicki-Hummer (RH) spectral synthesis code was utilized. The RH code is designed to model the formation of spectral lines in stellar atmospheres by solving the radiative transfer equation. This involves accounting for various atmospheric conditions, such as temperature, pressure, and magnetic fields, to accurately simulate the formation of spectral lines [27].

3.4.3 Processing MURaM Data Cubes with RH Code

A total of 11 MURaM data cubes, representing sequential time steps, were processed using the RH code. This processing allowed for the creation of synthetic spectral lines that closely mimic those observed in the Sun. By comparing these synthetic lines with actual observations, it is possible to gauge the accuracy of the MURaM simulations and make necessary adjustments. This step is essential for ensuring the reliability of the simulations in representing real solar phenomena and contributes to the broader goal of understanding solar magnetic activity and its impact on solar irradiance [28].

3.5 Degradation of Synthetic Spectra

The process of degrading synthetic spectra involves several steps to ensure that the simulated data closely resembles what is observed through the instruments aboard Sunrise, particularly the IMaX. This process is vital for validating the simulation results against actual observations.

3.5.1 Modeling Instrumental Effects

A custom Python class was developed to handle the Synthetic Sunrise data. This involved:

1. **Data Processing**: The RH output files were ingested to produce a comprehensive data array.

2. **Normalization**: The mean continuum intensity of each synthetic image was computed. Each image was then normalized by dividing it by its mean continuum intensity.

3. **Artificial Diffusion Correction**: To mitigate the effects of artificial diffusion from the MURaM simulation's numerical grid, a 2x2 convolutional kernel was applied. This kernel averaged every four adjacent pixels, enhancing the image quality and making the simulation more representative of real solar observations.

3.5.2 Spectral Degradation and Wavelength Sampling

To align the synthetic spectra with the spectral resolution of the IMaX instrument:

1. **Initial Resolution**: The synthetic spectra started with a resolution of 10 mÅ.

2. **Convolution with Gaussian Function**: The spectra were convolved with a Gaussian function having a Full Width at Half Maximum (FWHM) of 85 mÅ to emulate IMaX's spectral resolution.

3. **Wavelength Sampling**: After convolution, the spectra were sampled at the specific wavelengths used by IMaX, reducing the spectral lines to five distinct data points [29].

3.5.3 Accounting for the Spatial Point Spread Function

The IMaX image reconstruction process already compensates for the effects of the telescope's finite aperture and central obstruction. Therefore, it was not necessary to replicate these factors in the simulations. Instead, a low-pass filter was applied to the simulated images to eliminate power beyond the Sunrise telescope's cut-off frequency k_c, ensuring that the simulated data matches the observational limitations of the telescope [16].

4 Results

4.1 Analysis of Sunrise Data

4.1.1 Downsampling to PSPT Resolution

To facilitate a comparative analysis between the high-resolution Sunrise data and the PSPT observations, it was essential to downsample the Sunrise images (0.05"/pixel) to match the lower resolution of the PSPT data (1"/pixel). This process involved a two-step approach: smoothing via a Gaussian filter followed by downsampling using the Fast Fourier Transform (FFT) method.

Gaussian Smoothing Initially, each Sunrise image was subjected to a Gaussian filter. This smoothing operation helps in reducing high-frequency noise and mitigating the effects of fine-scale solar features that would be unresolved in the PSPT data. The Gaussian filter's standard deviation, denoted by $\sigma = 8$, was carefully chosen to preserve the overall structure while ensuring a smooth transition to lower resolutions.

FFT-Based Downsampling Following the smoothing step, the FFT was applied to transform the spatial data into the frequency domain. By centering the zero-frequency component and selectively retaining the lower-frequency components, we effectively mimicked the PSPT's resolution. This was achieved by applying a mask that zeroes out higher frequencies beyond a certain threshold, determined by the desired downsample factor. The inverse FFT was then used to transform the frequency-domain data back into the spatial domain, resulting in a downsampled image that closely resembles what would be observed by PSPT.

Implementation The downsampling process was implemented in Python, leveraging the *gaussian_filter* function for smoothing and the *fftn*, *fftshift*, *ifftshift*, and *ifftn* functions from NumPy for the FFT-based downsampling. This method ensured that the downsampled

Sunrise data maintained the integral characteristics necessary for an accurate comparison with PSPT observations.

The effectiveness of this approach, which can be seen in Figure 6, allowed us to analyze the Sunrise data under similar observational constraints as the PSPT, providing a robust basis for comparing the two datasets.

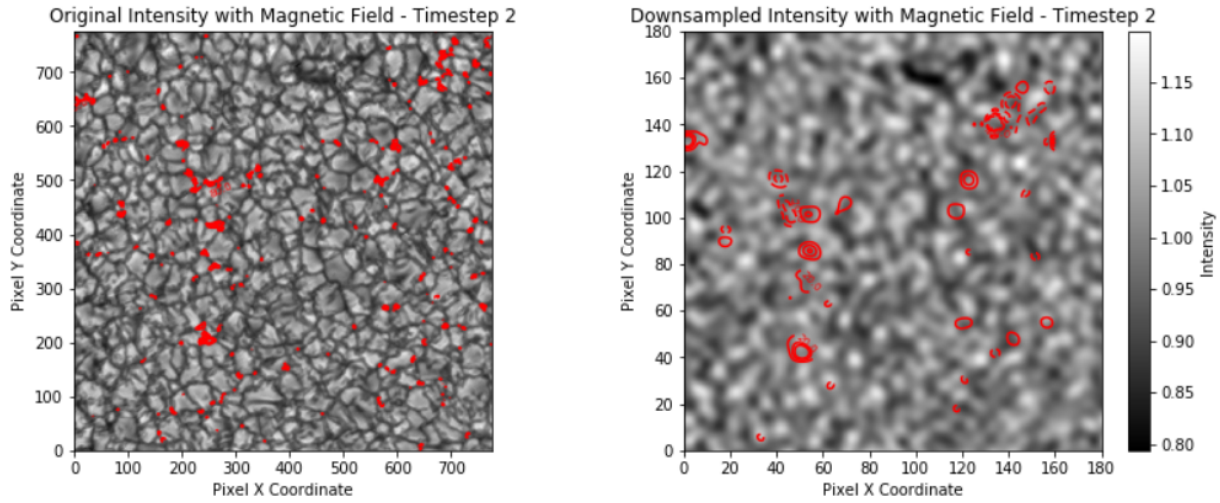

Figure 6: A comparative visual assessment of implementing this downsampling function to match the resolution of Sunrise 1 Data with PSPT's Resolution. The intensity map is in grayscale with red contours showcasing the magnetic field magnitude.

4.1.2 Results from of downsampled data analysis

The comprehensive analysis involved 42 timesteps of solar data from Sunrise 1, with an emphasis on understanding the relationship between magnetic field strength and solar intensity.

Methodological Approach The spatial resolution of 1 arcsec/pixel, equivalent to approximately 280 km/pixel, allowed for the detailed examination of the photospheric conditions. The Disk-center emergent intensity at $\lambda = 500$ nm was plotted against the absolute value of the magnetic field strength using a tailored Python script. The script's functionality included

percentile-based filtering (1st to 99th) to focus on the most representative data points, as seen in Figure 7.

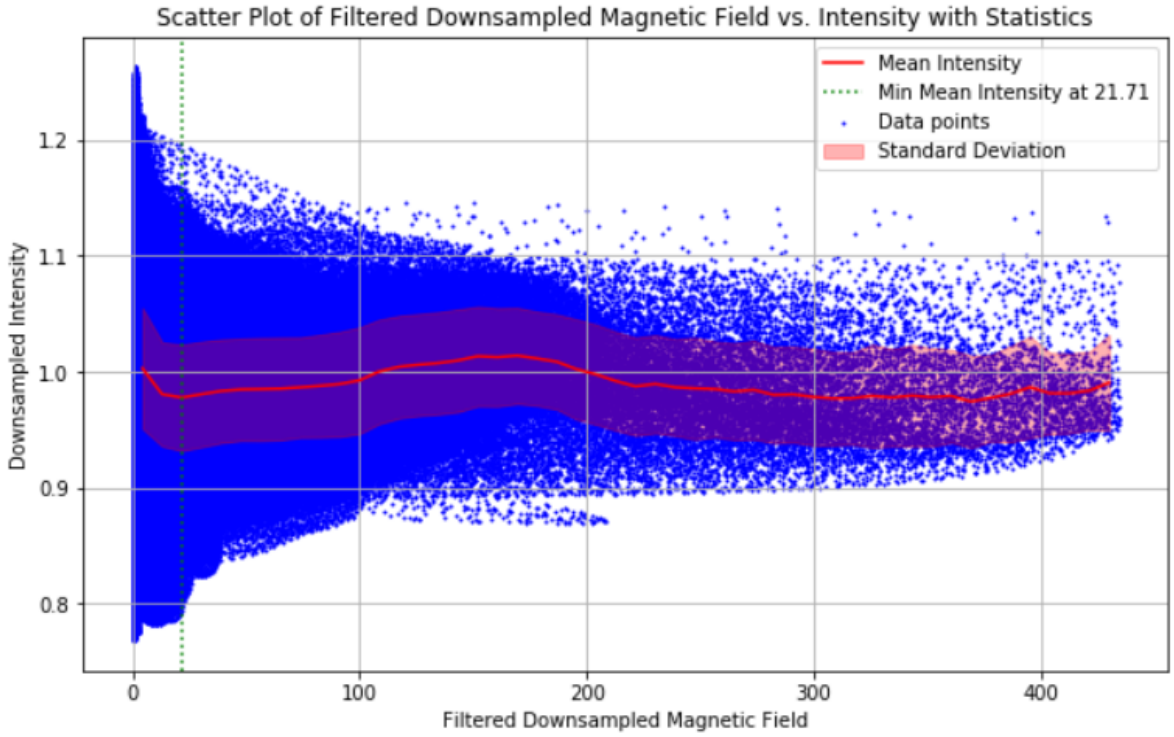

Figure 7: Disk-center emergent intensity at $\lambda = 500$ nm as a function of magnetic field strength. The 20 G threshold marks the onset of significant magnetic structuring.

Data Analysis Techniques Pixels exhibiting negligible magnetic flux density, approximately 0 G, are typically situated at the core of granulation patterns and tend to exhibit a marginally higher brightness compared to adjacent areas [30]. As the absolute value of the magnetic flux density increases, it generally signifies the commencement of magnetic field accumulation within the plasma downflow lanes. When the magnetic flux density surpasses roughly 20 G, there is an observed uptick in the average emergent intensity; such values are indicative of locations within magnetic features where the magnetic field strength escalates.

Utilizing the Python libraries NumPy and SciPy, statistical analyses were conducted on the filtered data to determine the average and standard deviation of the intensity within each magnetic field strength bin. A key finding was the 20 G threshold, where the mean

intensity started to rise, indicating the formation of magnetic structures.

Visualization and Mapping To visualize the spatial distribution of magnetic structures, masks were applied to the magnetic field data using morphological operations to enhance the clarity of structures. This was followed by categorizing spatially adjoining regions that met the criteria for magnetic structures, as depicted in Figure 8.

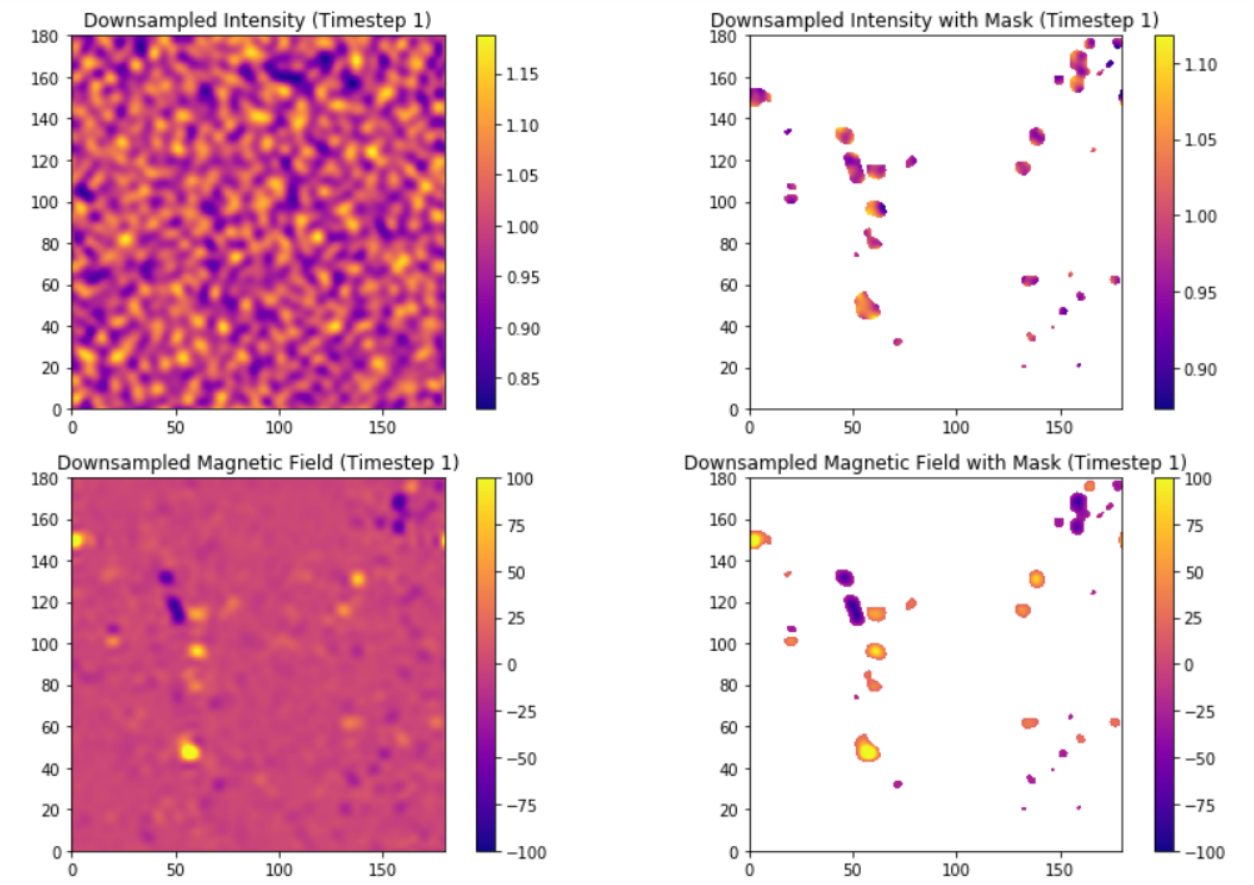

Figure 8: Applying a magnetic flux threshold to identify and visualize magnetic structures at timestep 1 of the downsampled Sunrise image

Statistical Distributions A series of histograms were generated to represent the statistical distribution of fractal widths, mean magnetic field strengths, and intensities. These histograms, shown in Figure 9, were instrumental in discerning the prevalent characteristics of magnetic structures in this dataset.

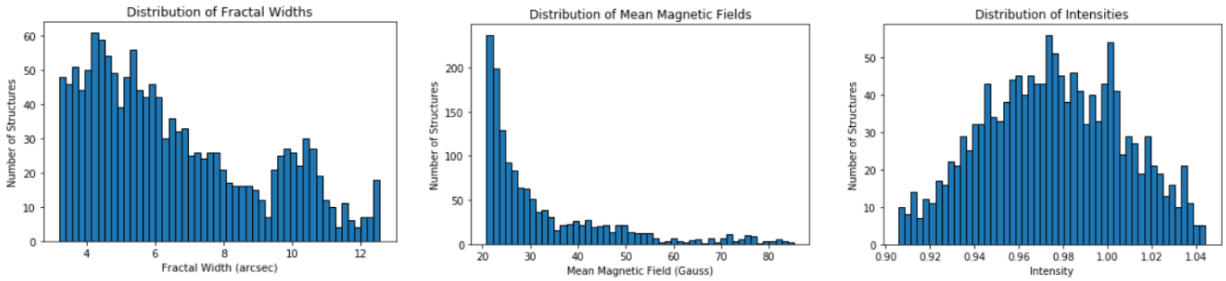

Figure 9: Histograms depicting the distribution of fractal widths, mean magnetic field strengths, and intensities for the identified structures in the downsampled Sunrise dataset.

Correlational Analysis A three-dimensional scatter plot was constructed to highlight the relationship between intensity and fractal width, with the color coding representing the mean magnetic field strength. This plot, seen in Figure 10, reveals a clear correlation between structure size and magnetic field strength.

4.2 Analysis of PSPT data

4.2.1 Contrast, Alignment, and Trimming

The initial phase of analyzing the PSPT data involved a series of preprocessing steps to enhance image quality and ensure consistency across the dataset. This process was crucial for the accurate assessment of solar features and involved contrast enhancement, alignment of images, and trimming to focus on the central, undistorted region of the solar disk.

Contrast Enhancement and Alignment Using IDL (Interactive Data Language), the contrast of the PSPT images was enhanced to better distinguish solar features such as sunspots, faculae, and granulation patterns. The images captured in the red (R), blue (B), and Ca II K (K) filters were processed separately. Each image underwent a contrast-limited adaptive histogram equalization (CLAHE) to improve the visibility of features without introducing artifacts.

Following contrast enhancement, the images were aligned to correct for any rotational or translational misalignments that occurred during observation. This alignment ensured

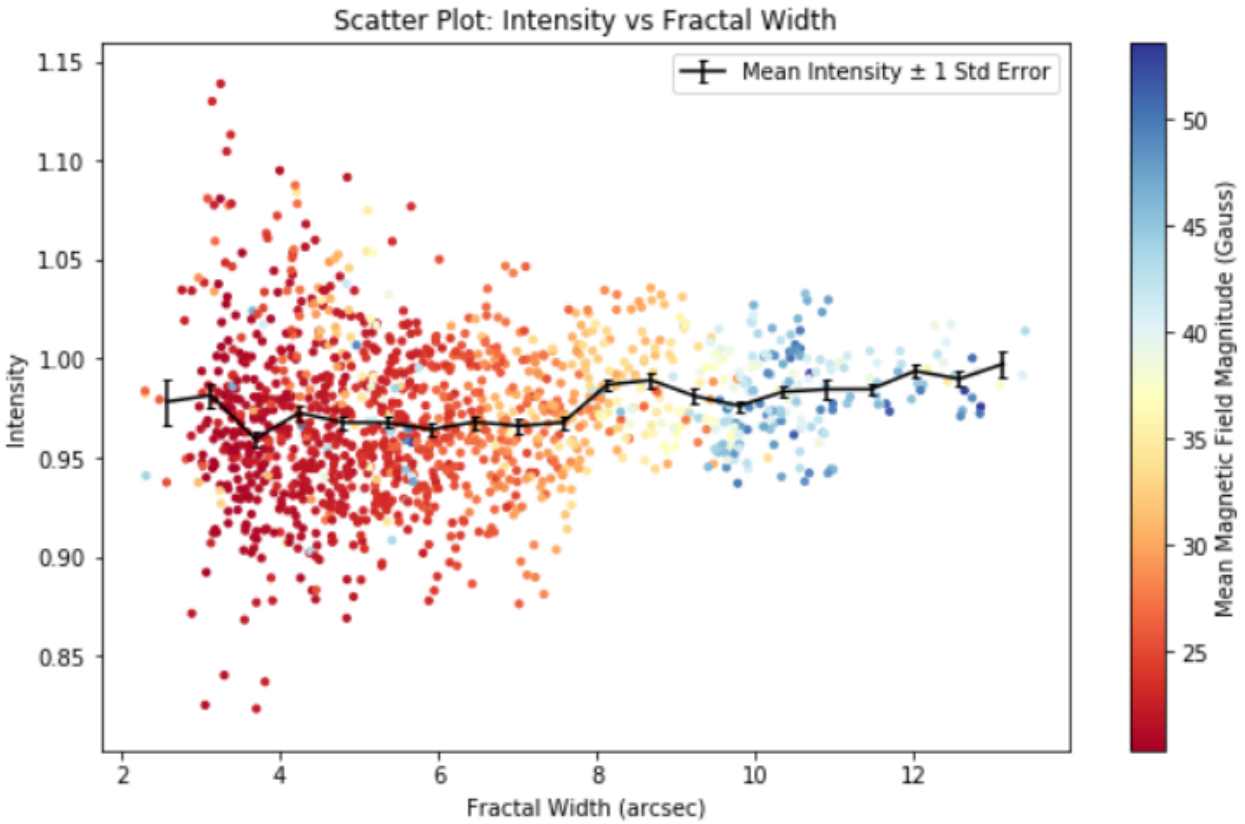

Figure 10: Scatter plot of intensity versus fractal width for identified structures in the downsampled Sunrise dataset, color-coded by mean magnetic field strength.

that corresponding features across the R, B, and K images were co-located, facilitating a coherent analysis of multi-wavelength data. The alignment was achieved using a cross-correlation technique, which identifies the best fit between image pairs by maximizing the similarity measure.

Trimming to Central Region After enhancing and aligning the images, the next step was to trim them to a central region of 180x180 pixels. This trimming was performed in Python and focused on the undistorted central area of the solar disk, which is least affected by projection effects and atmospheric distortion near the limb. The choice of this specific region was dictated by the need to analyze the most reliable and representative part of the image, ensuring that the subsequent analysis was based on high-quality, consistent data.

The trimmed images provided a standardized dataset for a detailed examination of solar

features and their variations. By concentrating on the central portion of the solar disk, we minimized the impact of edge distortions and ensured that the analysis was grounded in the most accurate representation of solar activity available in the PSPT data.

4.2.2 K-filter as Magnetic Field Proxy

The sensitivity of the Ca II K-line emission to magnetic fields, especially in the solar chromosphere, underpins its use as a proxy for mapping magnetic activity. The Ca II K-line's response to the solar magnetic field enables us to infer magnetic field strengths from the chromospheric features it highlights.

Empirical Relationship A key aspect of our methodology is the conversion from proxy data to estimations of the actual magnetic field. This conversion relies on an empirical relationship, which is established by comparing the intensity of Ca II K-line features against direct magnetic field measurements from magnetograms. The relationship is quantified by the formula:

$$\left(\frac{\delta I}{I_{qs}}\right)_K = 0.016 \left(\frac{B}{\mu}\right)^{0.66}$$

where $\left(\frac{\delta I}{I_{qs}}\right)_K$ represents the contrast in the K-line emission relative to the quiet Sun, B is the magnetic field strength, and μ denotes the cosine of the angle between the line of sight and the normal to the solar surface.

Calibration and Validation This proxy-to-real magnetic field conversion formula has undergone rigorous calibration and validation using datasets that offer both Ca II K-line intensity measurements and corresponding direct magnetic field observations. The calibration process ensures that our formula accurately reflects the underlying physics, while validation against independent datasets confirms its reliability [31].

Visualization of Magnetic Fields The practical application of this formula is demonstrated by overlaying contours of calculated magnetic field strengths on intensity maps. As seen in the accompanying Figure 11, red contours delineate areas of intense magnetic activity, such as sunspots. The correlation between these contours and the sunspot's known magnetic field serves as evidence of the method's effectiveness in tracing magnetic fields.

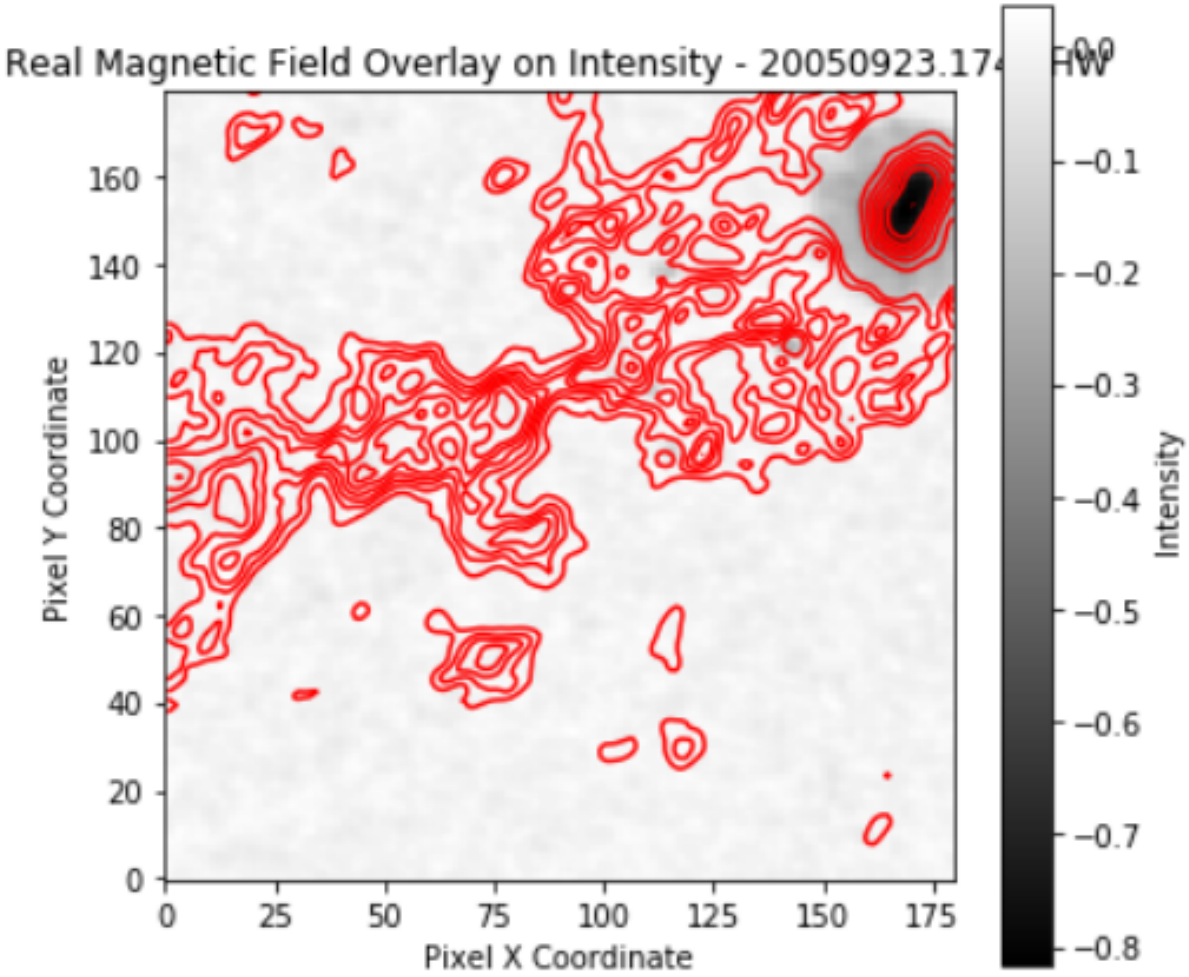

Figure 11: Red contours created using our formula highlight the sunspot, showing that our method effectively traces the sunspot's magnetic field.

This innovative approach, grounded in empirical data, enhances our ability to study solar magnetism in regions where direct magnetic field measurements may not be available. It also offers a pathway to retrospectively analyze historical data, providing insights into solar

magnetic activity trends over longer periods than direct measurements permit.

4.2.3 Results from PSPT Data Analysis

With the Sunrise data adjusted to match the resolution of the PSPT dataset, a parallel analysis was performed on the PSPT images. This approach allowed for a direct comparison between the two data sets, focusing on the relationship between solar magnetic activity inferred from the Ca II K-line intensity and solar irradiance.

Methodological Approach The PSPT images, captured at a resolution of 1 arcsec/pixel, provided a broad view of solar activity. The emergent intensity in the PSPT data, as seen at $\lambda = 500$ nm, was compared with the magnetic field values produced from the conversion equation and magnetic field proxy obtained from the Ca II K-line intensities. For this analysis, a Python script was utilized to examine the relationship between the magnetic proxy values and solar intensity, ensuring consistency with the approach taken for the Sunrise data.

The relationship between the Magnetic Field and Intensity was plotted to establish a threshold of significance for magnetic field presence, which is shown in Figure 12.

Visualization and Mapping To visualize the spatial distribution of the inferred magnetic structures, the same morphological operations applied to the Sunrise data were used on the PSPT images. A trial-and-error approach led to the adoption of a 20 G threshold (consistent with the threshold from Sunrise analysis) to identify significant magnetic features. This threshold, while not immediately apparent from the initial scatter plot, proved effective in subsequent mask applications, as shown in Figure 13.

Statistical Distributions The PSPT data facilitated the generation of histograms to statistically describe the identified magnetic structures in terms of their size, magnetic field proxy strength, and intensity. These histograms, presented in Figure 14, are instrumental in

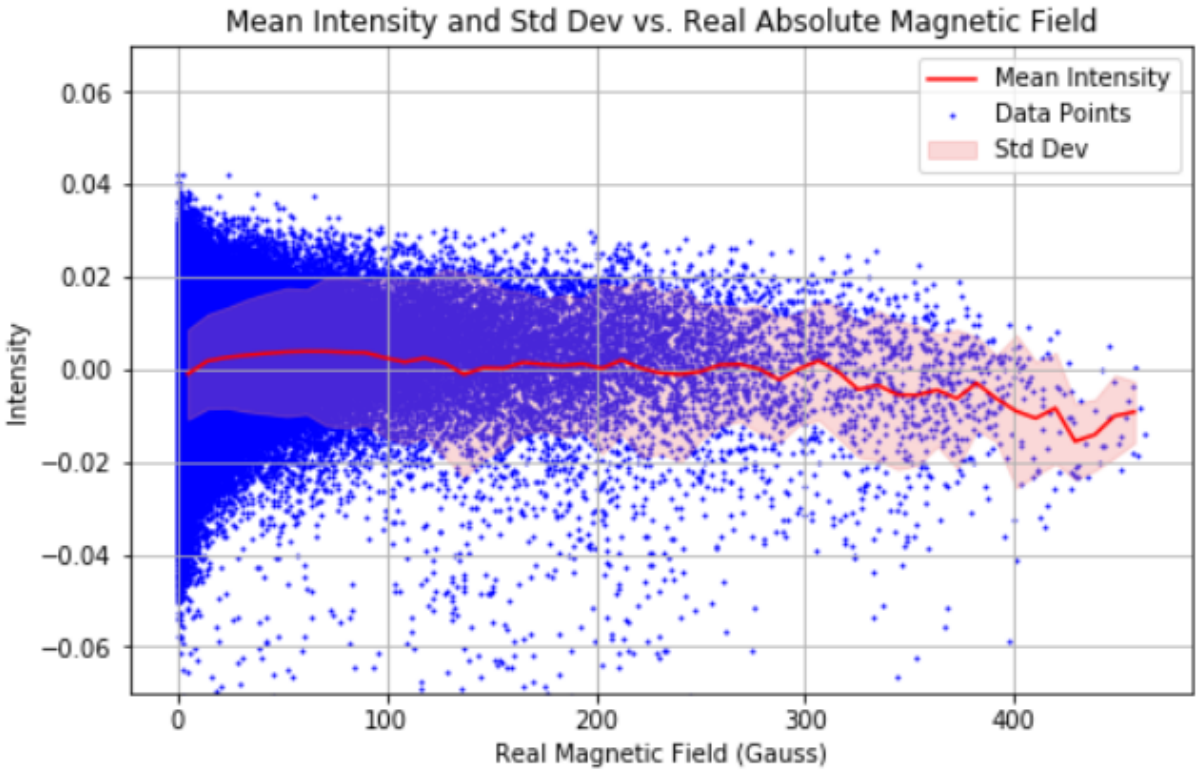

Figure 12: Threshold couldn't be chosen using this scatter plot as the location of the minimum mean intensity is not obvious here. Instead, a threshold was chosen through trial and error with several values in the mask.

discerning the properties and distributions of magnetic activity across the solar disk.

Correlational Analysis A three-dimensional scatter plot was created to elucidate the relationship between intensity and fractal width, with color coding indicative of the average magnetic proxy values. This scatter plot, presented in Figure 15, demonstrates a correlation between the size of the structures and the inferred magnetic field strength, mirroring the findings from the downsampled Sunrise dataset.

The analysis of PSPT data, while initially challenging due to the absence of a clear threshold from scatter plots, benefitted immensely from a systematic approach in selecting an effective magnetic field strength threshold. The consistency of the 20 G threshold across different datasets not only substantiates the analysis techniques employed but also confirms the reproducibility of results, which is crucial for validating solar magnetic field studies.

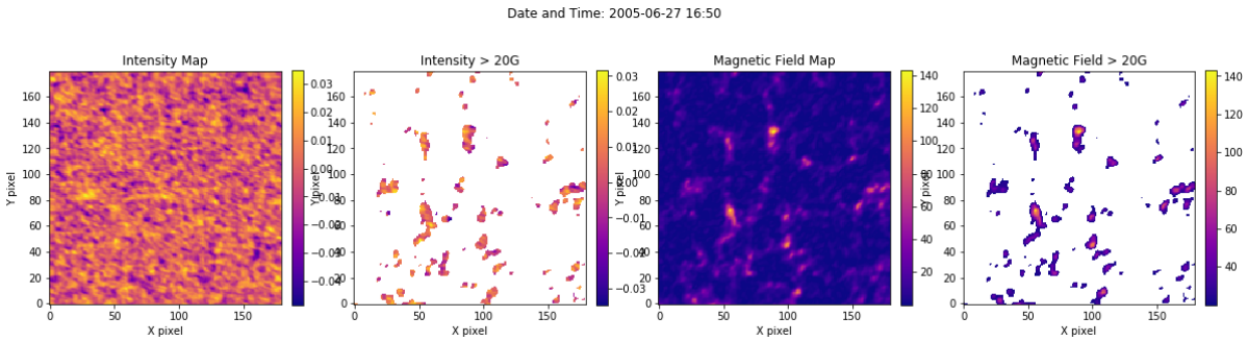

Figure 13: Mask is applied to all pixels with an unsigned vertical magnetic flux greater than 20 G. Using this mask, we identify a magnetic structure as any collection of 10 or more pixels that are spatially adjoined.

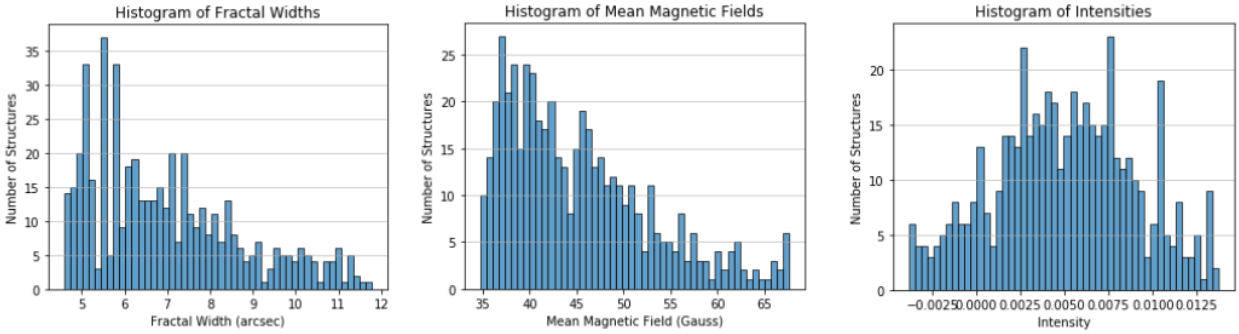

Figure 14: These histograms are indicative of larger structures harboring stronger magnetic fields. This makes sense if we consider that larger solar features such as sunspots are areas of intense magnetic activity, and thus, larger structures would be expected to show higher magnetic field values.

4.3 Analyis of MURaM Synthesized Spectra

The validation of numerical simulations against observational data is an important step in understanding solar phenomena. This section presents a rigorous analysis of 11 images generated from synthesized spectra using the MURaM simulation framework, compared with data from observations.

4.3.1 Data Preparation and Degradation

The synthesized images, designed to replicate the conditions captured by Sunrise, were processed to emulate instrumental effects. This process detailed in Subsection 3.4 is critical

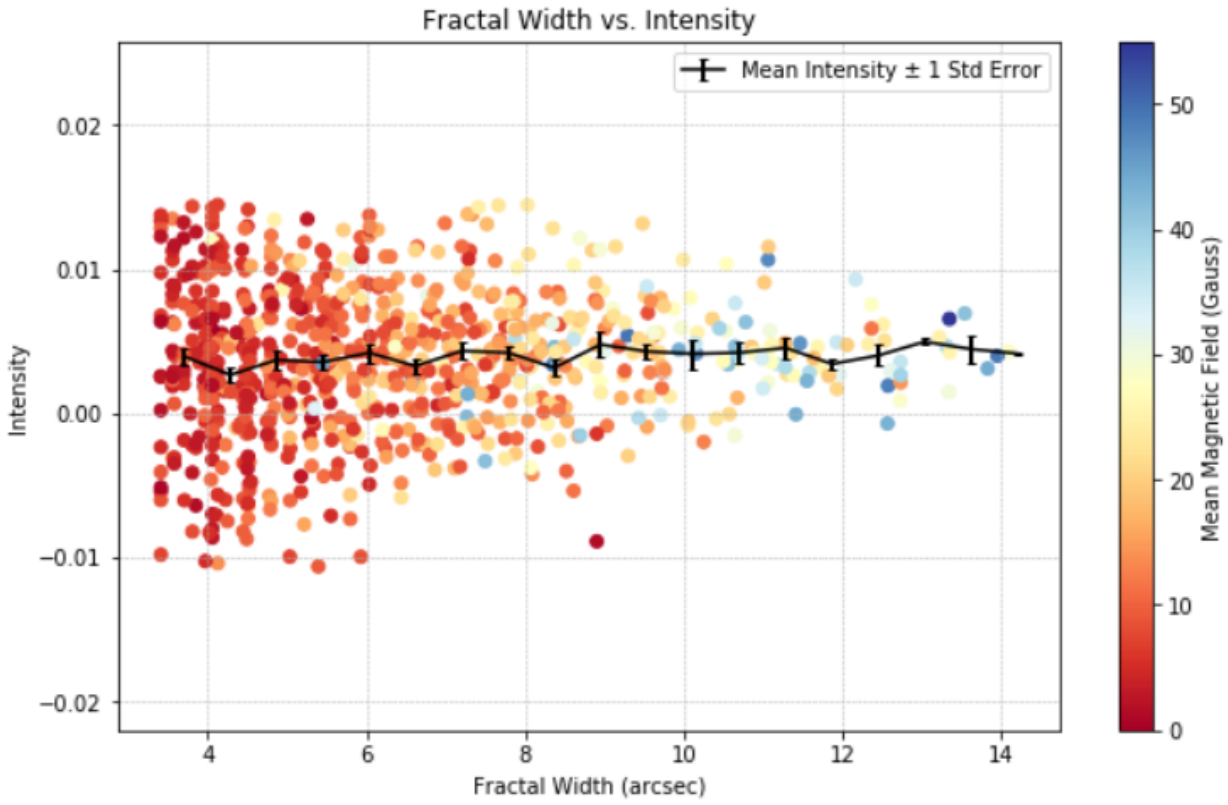

Figure 15: This scatter plot with overlaid line graph shows the relationship between fractal width in arcseconds and intensity of solar features, with color indicating the mean magnetic field strength in Gauss. The line with error bars represents the mean intensity with its standard error of the mean, providing a trend that considers the dispersion of the data.

for ensuring the synthetic data's fidelity to real-world observations.

4.3.2 Comparison with Downsampled Observational Data

Upon the successful preparation and degradation of synthesized spectra to mirror Sunrise conditions, a subsequent step involved downsampling these data to match the PSPT resolution, which is highlighted in Subsubsection 4.1.1. This comparison is crucial for bridging the gap between high-resolution simulations and lower-resolution observations, which capture global solar phenomena.

Methodology The downsampling of MURaM synthesized spectra was conducted using a Gaussian filter to smooth the data, followed by a Fourier Transform to capture the spectral

content. A low-pass filter was then applied to eliminate high-frequency components, reflecting the resolution and observational constraints of the PSPT. This method ensured that the resulting synthetic images were directly comparable to the PSPT data.

Analysis of Downsampled Synthetic Data The downsampled synthetic data were subjected to the same analytical processes as the observational data. The intensity at $\lambda = 500$ nm was mapped against the synthetic magnetic field values. The derived relationships were indicative of the veracity and reliability of the MURaM simulations in reproducing solar magnetic features observable with PSPT.

Ensuring Consistency Across Data Sets In comparing the downsampled synthetic data with PSPT observations, particular attention was paid to maintaining consistency in methodology. The same scripts and thresholding techniques applied to the observational data were employed here, enabling a robust comparison between the synthetic and observational datasets.

Results from Downsampled Synthetic Data Analysis The analysis revealed correlations between the synthesized magnetic field strengths and intensities, akin to those discovered in the PSPT data. Histograms and scatter plots, analogous to those produced for the observational data, demonstrated the capacity of the MURaM simulations to accurately capture the trends and distributions of solar magnetic activity. These results, which are detailed in Figures 16, 17, 18, and 19, underscore the effectiveness of simulations in supplementing and extending our knowledge derived from solar observations.

The validation process, highlighted by the congruence of findings between downsampled synthetic and PSPT observational data, not only confirms the robustness of the MURaM model but also enhances confidence in the use of synthetic data for exploring broader solar phenomena beyond the reach of current observational capabilities.

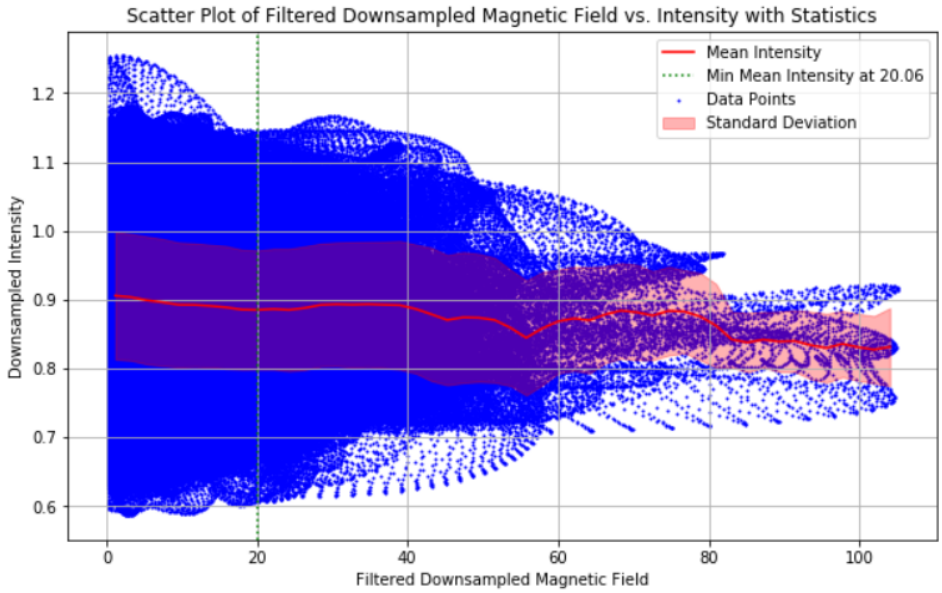

Figure 16: Threshold value of 20 G was chosen based on the location of the minimum mean intensity and represents the pixels where the magnetic field has begun to concentrate in the downflow lanes to form magnetic structures.

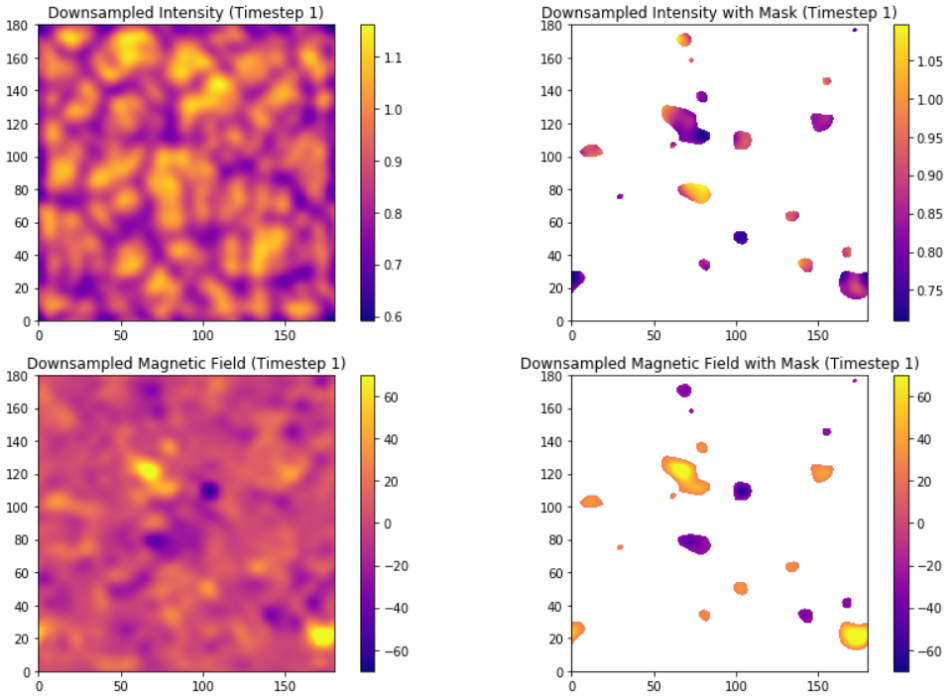

Figure 17: Mask is applied to all pixels with an unsigned vertical magnetic flux greater than 20 G. Using this mask, we identify a magnetic structure as any collection of 10 or more pixels spatially adjoined.

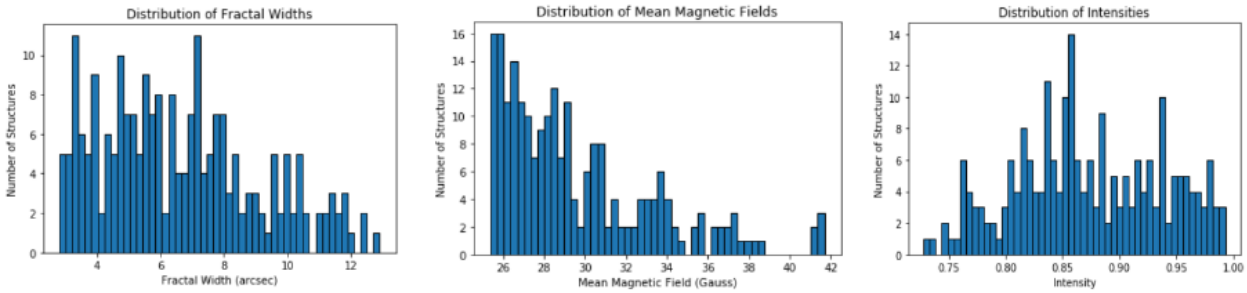

Figure 18: Histograms illustrating the statistical properties of magnetic structures within the downsampled synthetic data.

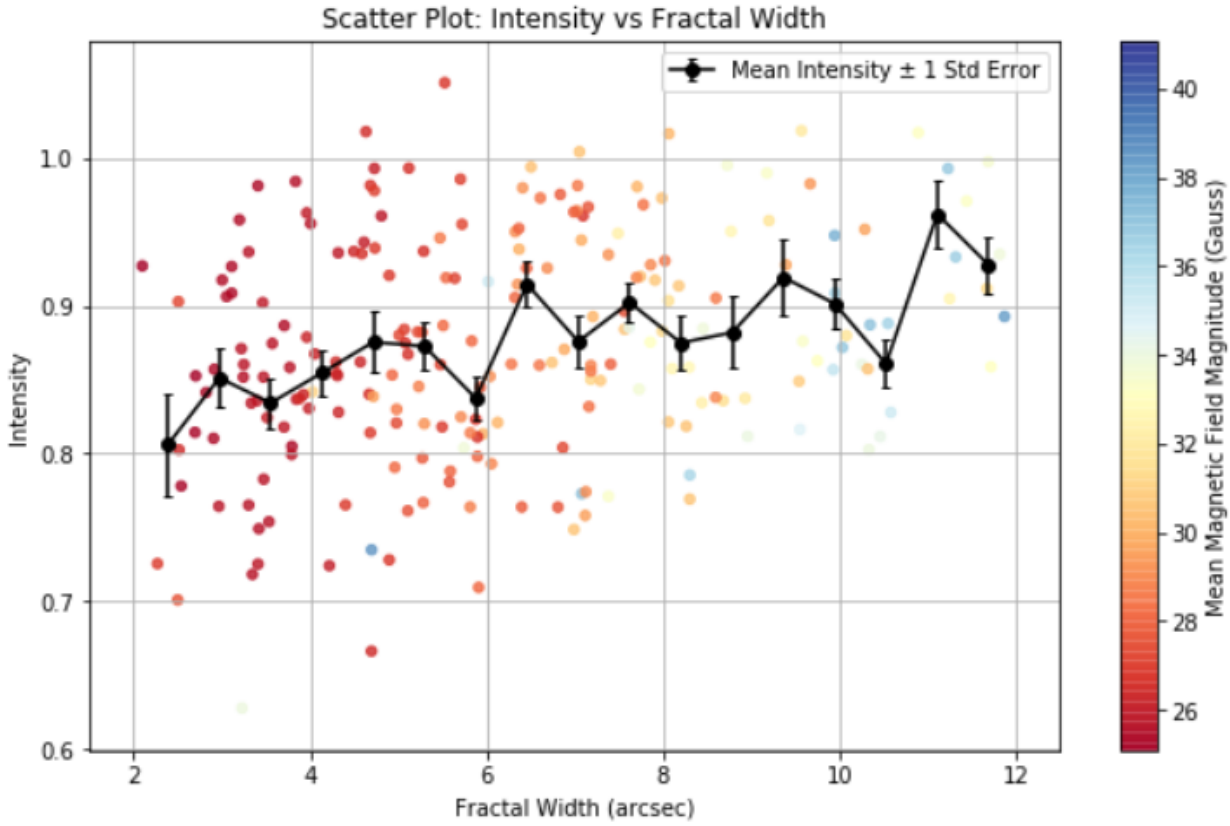

Figure 19: Scatter plot correlating the fractal width and intensity of synthesized solar features, with the mean magnetic field strength depicted by color gradients.

5 Discussion

5.1 Comparative Analysis of Observational and Synthesized Data

The integration of observational data with numerical simulations from MURaM has afforded a deeper insight into the complex nature of solar magnetic fields. The methodologies, while consistent across different datasets, have unraveled a clear correlation between the size of solar features and their magnetic field strengths. This relationship is discernible within both the high-resolution observations from the Sunrise I observatory and the expansive full-disk images from the PSPT, as well as in the synthetic datasets produced by MURaM simulations.

Divergences Between Data Types While the analyses of observational and synthetic datasets demonstrate congruent trends concerning the size and magnetic field strength of solar features, the direct effects on solar irradiance intensity remain ambiguous. The nuanced differences between these datasets emphasize the complexity of magnetic fields and emitted solar radiation and point to the need for further investigation into this relationship.

The Critical Role of Data Processing The methodical degradation of synthetic spectra to emulate the observational resolution is a testament to the difficult and complex process required for meaningful data comparison. This meticulous approach reinforces the validity of simulations in replicating real solar phenomena, highlighting the necessity of precision in considering instrumental and observational constraints.

5.2 Caveats and Considerations

The conclusions drawn from this research are promising; however, they are not without their caveats. The inherent assumptions in the MURaM simulations, coupled with the limitations of observational instrumentation, introduce constraints that necessitate cautious

interpretation of the findings. Moreover, the reliance on magnetic flux thresholds for structure identification in both synthetic and observational datasets underscores the need for ongoing refinement and validation of these analytical techniques.

5.3 Future Avenues for Research

Augmenting Data Fidelity Future endeavors should focus on expanding the collection of synthetic images and incorporating observations from cutting-edge solar telescopes such as DKIST. This expansion would provide a richer dataset for analysis, facilitating a more granular understanding of solar magnetic dynamics. Moreover, fostering collaborations with the wider research community would be invaluable in cross-validating findings and fostering a comprehensive understanding of solar phenomena.

Enhancement of Analytical Methodologies Subsequent research should explore more sophisticated methods for identifying and analyzing magnetic structures. Prolonged observational missions, accompanied by a broadened scope for capturing diverse solar phenomena and refined parameters for simulations, are imperative for acquiring a holistic picture of the solar atmosphere's magnetic intricacies.

6 Conclusion

The pursuit of this research has significantly enhanced our comprehension of magnetic fields within the solar atmosphere. Analyses of high-definition Sunrise I data, expansive PSPT observations, and detailed MURaM synthetic spectra have collectively shed light on the nuanced dynamics of magnetic structures and their potential effects on solar irradiance.

Significance and Broader Implications Our study stands as a meaningful contribution to solar physics, helping our understanding of the behavior of magnetic fields in the solar photosphere and underscoring their significance in space weather prediction and solar-terrestrial interactions. These findings have far-reaching implications, from the technical spheres of satellite operation and communication to the broader context of Earth's climatic systems.

Synthesis and Prospects We have discerned a distinct correlation between the size of solar structures and their magnetic potency; however, the impact on solar irradiance intensity remains to be fully elucidated. The current dataset and analytical methods, while robust, call for further expansion and refinement. The process of degrading synthetic data underscores the paramount importance of accounting for observational limitations and highlights the value of simulations in extending our observational reach.

In closing, our research lays the groundwork for future studies and offers a fundamental insight into the complex magnetic mechanisms of our nearest star. The methodologies honed and insights gleaned herein significantly contribute to the collective scientific endeavor to decode the Sun's influence and serve as a stepping stone for future explorations in solar physics.

References

[1] K. J. H. Phillips. *Guide to the Sun*. Cambridge University Press, 1992.

[2] J. N. Bahcall. *Neutrino Astrophysics*. Cambridge University Press, 1995.

[3] P. Charbonneau. "Dynamo models of the solar cycle." *Living Reviews in Solar Physics*, vol. 7, no. 1, 2010.

[4] D. K. Lynch, and G. A. Chapman. "Solar granulation and oscillations as spatially random processes." *Astrophysical Journal*, vol. 197, Apr. 1, 1975, pt. 1, p. 241-249.

[5] Å. Nordlund, R. F. Stein, and M. Asplund. "Solar surface convection." *Living Reviews in Solar Physics*, vol. 6, no. 2, 2009.

[6] M. Ossendrijver. "The solar dynamo." *Astronomy and Astrophysics Review*, vol. 11, 2003, pp. 287-367.

[7] S. K. Solanki. "Sunspots: An overview." *Astronomy and Astrophysics Review*, vol. 11, 2003, pp. 153-286.

[8] D. H. Hathaway. "The solar cycle." *Living Reviews in Solar Physics*, vol. 7, no. 1, 2010.

[9] P. Foukal. "Solar Astrophysics." Wiley-VCH, 2004.

[10] L. J. Gray, J. Beer, M. Geller, J. D. Haigh, M. Lockwood, K. Matthes, U. Cubasch, D. Fleitmann, G. Harrison, L. Hood, J. Luterbacher, G. A. Meehl, D. Shindell, B. van Geel, and W. White. "Solar influences on climate." *Reviews of Geophysics*, vol. 48, no. 4, 2010.

[11] A. Pulkkinen. "Space weather: Terrestrial perspective." *Living Reviews in Solar Physics*, vol. 4, no. 1, 2007.

[12] R. Schwenn. "Space weather: The solar perspective." *Living Reviews in Solar Physics*, vol. 3, no. 2, 2006.

[13] V. Bothmer, I. A. Daglis. "Space Weather: Physics and Effects." Springer-Verlag, 2007.

[14] P. Barthol, A. Gandorfer, S. K. Solanki, M. Schüssler, B. Chares, W. Curdt, W. Deutsch, A. Feller, D. Germerott, B. Grauf, K. Heerlein, J. Hirzberger, M. Kolleck, R. Meller, R. Müller, T. L. Riethmüller, G. Tomasch, M. Knölker, B. W. Lites, G. Card, D. Elmore, J. Fox, A. Lecinski, P. Nelson, R. Summers, A. Watt, V. Martínez Pillet, J. A. Bonet, W. Schmidt, T. Berkefeld, A. M. Title, V. Domingo, J. L. Gasent Blesa, J. C. del Toro Iniesta, A. López Jiménez, A. Álvarez-Herrero, L. Sabau-Graziati, C. Widani, P. Haberler, K. Härtel, D. Kampf, T. Levin, I. Pérez Grande, A. Sanz-Andrés, and E. Schmidt. "The Sunrise Mission." *Solar Physics*, vol. 268, no. 1, 2011, pp. 1-34.

[15] A. Vögler, S.Shelyag, M. Schüssler, F. Cattaneo, T. Emonet, and T. Linde. "Simulations of magneto-convection in the solar photosphere." *Astronomy and Astrophysics*, vol. 429, 2005, pp. 335-351.

[16] S. K. Solanki, P. Barthol, S. Danilovic, A. Feller, A. Gandorfer, J. Hirzberger, T.L.Riethmuller, M. Schussler, J.A.Bonet, V. Martınez Pillet, J. C. del Toro Iniesta, V. Domingo, J. Palacios,M.Knolker, N. Bello Gonzalez, T. Berkefeld, M. Franz, W. Schmidt, and A. M. Title. "Sunrise: Instrument, mission, data, and first results." *The Astrophysical Journal Letters*, vol. 723, no. 2, 2010, L127-L133.

[17] W. Dean Pesnell, B. J. Thompson, and P. C. Chamberlin. "The Solar Dynamics Observatory (SDO)." *Solar Physics*, vol. 275, no. 1-2, 2012, pp. 3-15.

[18] M. P. Rast, A. Ortiz, and R.W. Meisner. "Latitudinal variation of the solar photospheric intensity" *The Astrophysical Journal*, vol. 673, no. 2, 2008.

[19] T. Berkefeld, W. Schmidt, D. Soltau, A. Bell, H. P. Doerr, B. Feger, R. Friedlein, K. Gerber, F. Heidecke, T. Kentischer, O. v. d. Lühe, M. Sigwarth, E. Wälde, P. Barthol, W. Deutsch, A. Gandorfer, D. Germerott, B. Grauf, R. Meller, A. Álvarez-Herrero, M. Knölker, V. Martínez Pillet, S. K. Solanki, A. M. Title. "The Wave-Front Correction

System for the Sunrise Balloon-Borne Solar Observatory" *Solar Physics*, vol. 268, no. 1, 2011, pp. 103-123.

[20] N.A. Krivova, S.K. Solanki, and Y.C. Unruh. "Towards a long-term record of solar total and spectral irradiance." *Journal of Atmospheric and Solar-Terrestrial Physics*, vol. 73, no. 2-3, 2011, pp. 223-234.

[21] V.Martinez Pillet, J.C.del Toro Iniesta, A. Alvarez-Herrero, V.Domingo, J. A.Bonet, L.Gonzalez Fernandez, A. Lopez Jimenez, C. Pastor, J.L. Gasent Blesa, P. Mellado, J.Piqueras, B. Aparicio, M. Balaguer, E. Ballesteros, T.Belenguer, L.R. Bellot Rubio, T. Berkefeld, M. Collados, W. Deutsch, A. Feller, F. Girela, B. Grauf, R.L. Heredero, M. Herranz, J.M. Jeronimo, H. Laguna, R. Meller, M. Menendez, R. Morales, D. Orozco Suarez, G. Ramos, M. Reina, J.L. Ramos, P. Rodriguez, A. Sanchez, N.Uribe-Patarroyo, P.Barthol, A.Gandorfer, M.Knoelker, W.Schmidt, S.K.Solanki, and S. Vargas Dominguez. "The Imaging Magnetograph eXperiment (IMaX) for the Sunrise Balloon-Borne Solar Observatory." *Solar Physics*, vol. 268, no. 1, 2011, pp. 57-102.

[22] J. C. del Toro Iniesta. "Solar Polarimetry and Magnetic Field Measurements" *Astrophysics and Space Science Library*, vol. 259, 2001, pp. 183-184.

[23] I. Ermolli, K. Matthes, T. DudokdeWit, N. A. Krivova, K. Tourpali, M. Weber, Y. C. Unruh, L. Gray, U. Langematz, P. Pilewskie, E. Rozanov, W. Schmutz, A. Shapiro, S. K. Solanki, and T. N. Wood. "Recent variability of the solar spectral irradiance and its impact on climate modelling." *Atmospheric Chemistry and Physics Discussions*, vol. 13, no. 8, 2013, pp. 3945–3977.

[24] J. R. Kuhn, and R. Coulter. "The Precision Solar Photometric Telescope Project" *American Astronomical Society*, vol. 25, 1993, pp. 1302.

[25] R. F. Stein. "Solar Surface Magneto-Convection." *Living Reviews in Solar Physics*, vol. 9, no. 1, 2012.

[26] C. J. Schrijvera, K. Kauristieb, A. D. Aylwardc, C. M. Denardinid, S. E. Gibsone, A. Gloverf, N. Gopalswamyg, M. Grandeh, M. Hapgoodi, D. Heynderickxj, N. Jakowskik, V. V. Kalegaevl, G. Lapentam, J. A. Linkern, S. Liuo, C. H. Mandrinip, I. R. Mannq, T. Nagatsumar, D. Nandys, T. Obarat, T. P. O'Brienu, T. Onsagerv, H. J. Opgenoorthw, M. Terkildsenx, C. E. Valladaresy, and N. Vilmerz. "Understanding the Space Weather Environment." *Space Science Reviews*, vol. 198, no. 1-4, 2015, pp. 7-48.

[27] H. Uitenbroek. "Multilevel Radiative Transfer with Partial Frequency Redistribution" *The Astrophysical Journal*, vol. 557, no. 1, 2001, pp. 389-398.

[28] M. Rempel. "Radiative MHD simulation of sunspot structure." *Astronomical Society of the Pacific*, vol. 416, 2009, pp. 461-466.

[29] S. Jafarzadeh, S. K. Solanki, M. Stangalini, O. Steiner, R. H. Cameron, and S. Danilovic. "High-frequency Oscillations in Small Magnetic Elements Observed with Sunrise/SuFI" *The Astrophysical Journal Supplement Series*, vol. 229, no. 1, 2017.

[30] C. L. Peck, M. P. Rast, S. Criscuoli, and M. Rempel. "The Solar Photospheric Continuum Brightness as a Function of Mean Magnetic Flux Density. I. The Role of the Magnetic Structure Size Distribution." *The Astrophysical Journal*, vol. 870, no. 2, 2019, pp. 89.

[31] C. J. Schrijver, J. Cote, C. Zwaan, and S. H. Saar. "Relations between the Photospheric Magnetic Field and the Emission from the Outer Atmospheres of Cool Stars. I. The Solar CA II K Line Core Emission" *The Astrophysical Journal*, vol. 337, 1989, pp. 964–976.